ADVANCED PROCESS MODELS AND CONTROL STRATEGIES FOR ROTARY PRINTING PRESSES

By

G. Brandenburg
Technische Universität München
GERMANY

ABSTRACT

Digitally position controlled and synchronized AC motors which have replaced the former mechanical line shaft allow for advanced control strategies of rotary printing presses. New controls require new process models. The state of the art of tensile force , stress and strain in the web is revisited in Part 1 of the contribution and extended to the dynamic behavior of so-called partial cutting register errors (PCRE) which add up to the total cutting register error (TCRE) at the cutting cylinder. These equations allow for the reconstruction and measurement of rapid changes of the modulus of elasticity (Young's modulus) and the cross section of the web which occur in the case of reel changes on the run. The reconstructed signal can be used for feed-forward control of closed loop controls. Furthermore, the mathematical description of the so-called doubling errors between two printing units is presented. Their correlation with color register errors yields new insights into the printing process. Part II of the contribution is devoted to the web dynamics in systems of rollers with macro slip and so-called partial slip which are responsible for the generation of sustained cutting register errors. They are explained for a three roller system. The transition from micro to macro slip entirely switches the dynamic structure of the system. For a roller combination, where the web is pressed onto a steel roller by narrow rolls with very small axial areas of contact, partial slip between web and the steel roller is assumed. A "q-model" is developed as a first approach to explain the upstream travelling of disturbances. Herewith a new component is available which can serve to model the entire printing press in the future. The introduction of partial register errors has led to the design of a two-variable control of both the partial cutting register error and the tensile force in the same web span, which is dealt with in Part III. This control which does not require any additional mechanical effort, considerably reduces the paper waste and increases the economic efficiency of the printing press. Experiments with a modern commercial web offset press confirm the above theoretical results.

NOMENCLATURE

General remarks

- For linearization $u(x,t) = \overline{u}(x) + \tilde{u}(x,t)$ is introduced.
- Sometimes the area where the web is pressed to the roller is denoted as "nip" – immaterial whether the contact pressure is generated by clamping through a roller or by wrapping the web around a roller.
- Into the rectangular blocks of the block diagram the symbols of the appropriate transfer functions are depicted. The Laplace functions are mostly notated besides the block. Circles denote coefficients.
- Symbols specific for Section 7 are defined there.

A_e	cross section of the stress-free web
$A_{en-1,n}(x,t)$	cross section dependent on position x and time t in span $(n-1,n)$
$\overline{A}_e$	steady-state value of A_e, assumed as constant along the whole web length
A_{eEn}	cross section A_e at the input of nip n
E	elasticity modulus (Young's modulus) or doubling error (Fig. 5f)
$E_{n-1,n}(x,t)$	elasticity modulus dependent on position x and time t in span $(n-1,n)$
$\overline{E}_{n-1,n}$	steady-state value of $E_{n-1,n}(x,t)$, not constant along the whole web length
E_{En}	elasticity modulus at the input of nip n
$\tilde{E}_{12}$	doubling error between printing units 1 and 2, see equations Fig. 5f and Fig. 6
$F_{n-1,n}$	tensile web force in span $(n-1,n)$
$f_o = kf_u$	whole number multiple of f_u, $k = 1, 2, ..., n$
f_u	revolution frequency of a roller
$G_{e\omega k}$	equivalent transfer function of closed loop speed control of drive k
$k_{\alpha n}$	force transmission ratio
l_{1n}	free web length between nip 1 and n
$l_{n-1,n}$	free web length between nip $(n-1)$ and n
PCRE	partial cutting register error
s	Laplace operator
t	time
TCRE	total cutting register error
$T_{e\omega k}$	equivalent time constant of closed loop speed control of drive k
T_{G13}	time constant between nip 1 and 3 with macro slip of nip 2
$T_{n-1,n}$	time constant (or dead time) between nip $(n-1)$ and n
$T_{1,n}$	dead time between nip 1 and n
T_u	revolution time of a roller

$u(x,t)$	variable
$\overline{u}(x)$	steady state of u
$\tilde{u}(x,t)$	small deviation from steady state $\overline{u}$
$\hat{u}$	step amplitude of u
$\tilde{u}_\infty = \lim_{t\to\infty} \tilde{u}(t)$	new steady state after a transient.
$\overline{v}$	mean value of web transport velocity
v_{cn}	circumference velocity of nip n
x	position
$\tilde{Y}_{1n}$	color register or cutting register error between printing nips 1 and n
$\tilde{Y}^*_{1n}$	partial cutting register error between nips 1 and n
$z_{T(n-1),n}(x,t)$	transport disturbance dependent on position x and time t in span ($n-1,n$), due to changes of cross section and Young's modulus of the web
z_{TEn}	transport disturbance at the input of nip n
α	angle of wrap
β	angle of the area of adhesion
γ	angle of the area of micro slip
ε_{En}	strain at input of nip n
$\varepsilon_{n-1,n}$	total strain in web span $(n-1,n)$
$\varepsilon_{Fn-1,n}$	force dependent strain in web span $(n-1,n)$
$\overline{\varepsilon}_{n-1,n} = \overline{\varepsilon}_{Fn-1,n}$	steady-state strain in web span $(n-1,n)$
$\varepsilon_{Tn-1,n}$	transport dependent strain in web span $(n-1,n)$
$\sigma_{n-1,n}$	stress in web span $(n-1,n)$
ω	angular velocity
ω_k	actual value of angular velocity (speed) of drive k
ω_{kw}	reference value of angular velocity (speed) ω_k

INTRODUCTION

Many publications on longitudinal modeling of web production and web handling systems in the paper, plastics and textile industries are devoted to plants in which no information will be printed on the running web. One of the main requirements in these systems is to keep the web tensions within certain limits in order to achieve a smooth running of the web and to guarantee a defined quality of the final product. Hence tension control and decoupling strategies are the main issue.

In multicolor rotary printing presses, however, not only the web tensions have to be kept constant, but four or more colors must be congruently superimposed with high accuracy on the running web. This requires closed loop controls for the so-called register errors and high precision synchronization of the printing cylinders. In the past this was achieved by mechanical line-shafts. About 15 years ago these were replaced by electronic line shafts which consist of electronically synchronized, high dynamic and high accurate speed and angle controlled AC motors with digital control [1]. In comparison, virtually in all other

production lines in which printed information had not to be considered, the individual drive technology was already implemented in the seventies of the last century. The new technology provides the opportunity to design advanced control strategies for web tensions and register errors, which in turn require extended process models.

Not many publications discussing rotary printing presses are available, due to the tradition of the manufacturers to keep the know-how within the company and due to the lack of institutes for scientific research in this field. As the author has had the unique opportunity to co-operate with one of the most important manufacturers of rotary printing presses in the world over the last ten years, this paper can be devoted solely to rotary printing presses. Starting from the state of the art before 1999 (c.f. [2], [3], [4], [5], [6], [7], [8] and [9]) it presents new mathematical models for the web transport and a new method for cutting register controls which were developed during this time.

The paper is organized as follows. *Part 1* deals with the printing press in which idealized rollers or roller pairs are assumed with perfect force transfer between rollers and web. Extended models for web strain and tension will be discussed in Section 1. The close linkage of color register errors and the so-called doubling errors will be explained in Section 2 and a new model for partial cutting register errors is presented in Section 3. In section 4 total and partial cutting register errors are compared. Section 5 is devoted to the reconstruction of transport disturbances due to automatic reel changes. In *Part 2* specific properties of mechanical elements of printing presses are treated: non-ideal force transfer due to macro slip on rollers in section 6 and imperfect clamping of partial width guide rolls, the so-called q-model, in Section 7. New control strategies are presented in *Part 3*: Section 8 deals with a new cutting register control, which is based on a two-variable, decoupled, and simultaneous control of the tensile force and the partial cutting register error in a web span.

PART 1 IDEAL ROLLERS WITH MICRO SLIP

1. FORCE, STRESS AND STRAIN IN THE WEB

Functioning of a Rotary Offset Printing Press

First the operation principle of a commercial printing press is explained. The simplified scheme of Fig.1 is used. The paper web is unwound from the reel "-1" (AW) and is led to the infeed section, consisting of two dancing rollers (TW1 and TW2) and nip 0 (EW), which are provided to impress the force F_{01} to the web. The paper web runs through the four printing units DE1 to DE4 where four colors and water are transferred to it. Then the web is dried in the drier T and cooled in the chilling unit 5 (KE) consisting of several chill rolls wrapped by the web. Roller pair 6 (WE) represents the drawing roller of the turn over device where the paper is longitudinally cut into two or more separate ribbons of which one or more can be turned by turn bars. Then these ribbons are gathered one above the other to form a package of several layers which are led to a former (not illustrated in Fig. 1), via the draw roller 7 (TR), where they are folded in length direction. Finally they are cut by a cross cutter 8 (MZ), which consists of a cutting cylinder and a cutting blade. In adjoining sections (not illustrated in Fig. 1) the product is finished for dispatch.

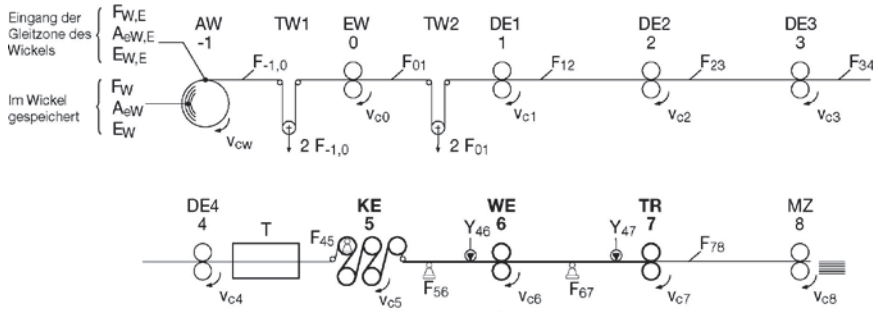

Eingang der Gleitzone des Wickels = Input line of area of micro slip of the reel
Im Wickel gespeichert = Stored in the reel

Figure 1 – Schematic view of a commercial offset printing press

Force, Stress and Strain

In this section equations are reviewed which are important for the later discussions. In many plants with moving webs electrically driven draw rollers are applied in order to transport the web and to control the tension in the web. As was shown in [2], [6] and [7] a roller 2 (see Fig. 2a and 3a) which is wrapped by a web impresses its circumferential velocity $\overline{v}_{c2}$ to the web in an area of adhesion $R_2\overline{\beta}_2$ at the input, where the tensile force in the web is $\overline{F}_2 = \overline{F}_{12}$. The bar on a variable denotes the steady-state operation. If $\overline{F}_{23} \neq \overline{F}_{12}$ is assumed in the adjacent down stream free web section, an area of slip $R_2\overline{\gamma}_2$ due to variable strain in the web develops on the roller, where $\overline{\gamma}_2$ satisfies the Euler-Eytelwein equation

$$\frac{\overline{F}_{23}}{\overline{F}_{12}} = \exp[\mu_2\overline{\gamma}_2 sign(\frac{\overline{F}_{23}}{\overline{F}_{12}} - 1)] \qquad \{1.1\}$$

and where the web velocity $\overline{v}$ differs from $\overline{v}_{c2}$, $\overline{v} \neq \overline{v}_{c2}$. For this type of slip the expression “micro slip” is introduced. As long as an area of adhesion exists, disturbances occurring in span 2-3 of the three roller system on Fig. 3a cannot travel in upstream direction: roller 2 is a “non-reactive” type.

Micro slip is assumed for any roller combination in Part 1 of this paper. Then the dynamic relationships are valid as presented in the following.

For the mathematical description of the moving web the continuity equation of continuum mechanics is fundamental. Adapting the general formulation to the web problem (see [3] and [4]) and subsequent linearization leads to the relation

$$\frac{1}{\overline{v}}\frac{\partial}{\partial t}\int_0^{l_{12}} \tilde{\varepsilon}_{12}(x,t)dx = \left[\tilde{\varepsilon}_{E1}(t) - \tilde{\varepsilon}_{E2}(t)\right] + \frac{\tilde{v}_{c2}(t) - \tilde{v}_{c1}(t)}{\overline{v}} \qquad \{1.2\}$$

which expresses that the difference of mass, which enters the control volume 1-2 at the input of nip 1 with velocity $\tilde{v}_{c1}(t)$ and strain $\tilde{\varepsilon}_{E1}(t)$, and the mass which leaves the control

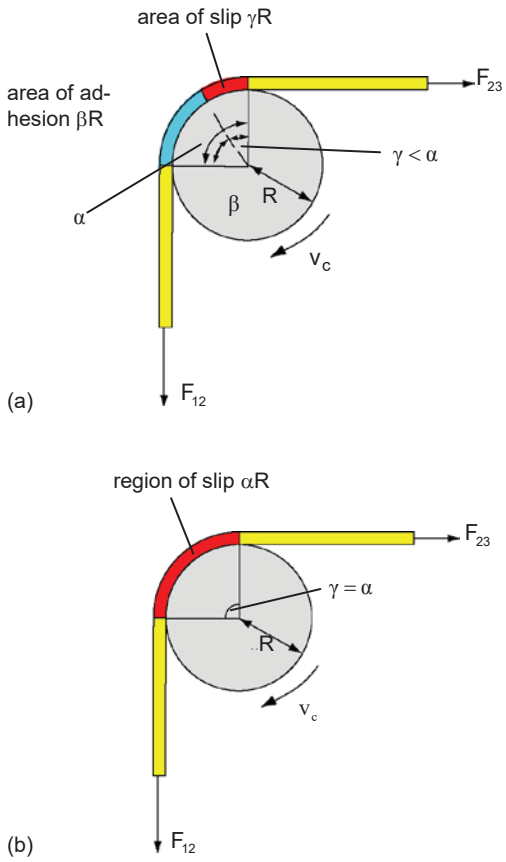

Figure 2 – Roller with micro slip (a) and with macro slip (b)

volume at the input of nip 2 with velocity $\tilde{v}_{c2}(t)$ and strain $\tilde{\varepsilon}_{E2}(t)$, changes the strain $\tilde{\varepsilon}_{12}(x,t)$ within the control volume.

In order to introduce stress and tensile force into {1.2}, Hooke's law is assumed to be constitutive for the web material. The well-known form of this law has to be generalized in order to consider a specific type of disturbances which occur in rotary printing presses.

During an automatic reel change the „new" web is pasted onto the „old" web which pulls the new web through the machine at rated transport speed. This involves a short-time change of the cross section of the web due to the splice together with virtually a step function of Young's modulus. These disturbances travel along the machine. Thus, cross section $A_{e12}(x,t)$ and Young's modulus $E_{12}(x,t)$ are dependent on position and time, whereas the web tensile force is only dependent on time. These web incorporated disturbances are shortly named "*transport disturbances*". Hooke's law takes the form [4]

$$\varepsilon_{12}(x,t) = \frac{F_{12}(t)}{A_{e12}(x,t)E_{12}(x,t)} \qquad \{1.3\}$$

Linearization for small deviations from the steady state

$$\bar{\varepsilon}_{12} = \bar{\varepsilon}_{F12} = \frac{\bar{F}_{12}}{\bar{A}_e \bar{E}_{12}} \qquad \{1.4\}$$

yields

$$\tilde{\varepsilon}_{12}(x,t) = \bar{\varepsilon}_{12}\left[\frac{\tilde{F}_{12}(t)}{\bar{F}_{12}} - \frac{\tilde{A}_{e12}(x,t)}{\bar{A}_e} - \frac{\tilde{E}_{12}(x,t)}{\bar{E}_{12}}\right] = \tilde{\varepsilon}_{F12}(t) + \tilde{\varepsilon}_{T12}(x,t) \qquad \{1.5\}$$

Mostly the cross section $\bar{A}_e$ may be assumed to be constant over the length of the web.

The transport disturbances induce deviations of tension, strain, color and cutting register errors when they are passing a nip. Because of the long distance between unwinder and folder the cutting register error (TCRE) can increase considerably, resulting in a high rate of paper waste. The color register errors are not significant in the case of commercial presses, but they are extremely important in the case of rotogravure presses. Newspaper printing is less critical.

These transport disturbances have been intensively discussed since the seventies of the last century and have been part of the mathematical model since then, see [4] and [6]. However, only during the last years progress was possible due to modern control techniques, see [10] and Section 5.

Three new variables are defined, the force dependent strain

$$\tilde{\varepsilon}_{F12}(t) = \bar{\varepsilon}_{12}\frac{\tilde{F}_{12}(t)}{\bar{F}_{12}} = \frac{\tilde{F}_{12}(t)}{\bar{A}_e \bar{E}_{12}} \qquad \{1.6\}$$

the transport dependent strain

$$\tilde{\varepsilon}_{T12}(x,t) = -\bar{\varepsilon}_{12}\left(\frac{\tilde{A}_{e12}(x,t)}{\bar{A}_e} + \frac{\tilde{E}_{12}(x,t)}{\bar{E}_{12}}\right) = -\bar{\varepsilon}_{12}\tilde{z}_{T12}(x,t) \qquad \{1.7\}$$

and the transport disturbance

$$\tilde{z}_{T12}(x,t) = \frac{\tilde{A}_{e12}(x,t)}{\bar{A}_e} + \frac{\tilde{E}_{12}(x,t)}{\bar{E}_{12}} \qquad \{1.8\}$$

In ideal steady-state of the press the web should be free of changes $\tilde{A}_e$ and $\tilde{E}$. Then $\tilde{\varepsilon}_{T12}(x,t) = 0$ and

$$\bar{\varepsilon}_{F12} = \bar{\varepsilon}_{12} \qquad \{1.9\}$$

hold. In reality small stochastic changes will occur.

Laplace transform of these equations yields for a system $(n-1, n)$, after long calculations similar to those in [4], the force dependent strain

$$\tilde{\varepsilon}_{Fn-1,n} = \frac{1}{1+T_{n-1,n}s}\left[\tilde{\varepsilon}_{Fn-2,n-1} + \left(\overline{\varepsilon}_{n-1,n} - \overline{\varepsilon}_{n-2,n-1}\right)\tilde{z}_{TEn-1} + \frac{\tilde{v}_{cn} - \tilde{v}_{cn-1}}{\overline{v}}\right] \qquad \{1.10\}$$

with the transport disturbance at the input of nip $(n-1)$:

$$\tilde{z}_{TEn} = e^{-T_{1n}s}\tilde{z}_{TE1} = e^{-T_{1n}s}\left(\frac{\tilde{A}_{eE1}}{\overline{A}_e} + \frac{\tilde{E}_{E1}}{\overline{E}_{01}}\right) \qquad \{1.11\}$$

where the transport delay is

$$T_{1n} = T_{12} + T_{23} + ...T_{i-1,i}... + T_{n-1,n} = \frac{l_{1n}}{\overline{v}} \qquad \{1.12\}$$

This is the dead-time which the transport disturbance needs to travel the distance l_{1n} from nip 1 to nip n with the mean velocity $\overline{v}$. Furthermore, the relationships

$$\overline{\varepsilon}_{n-1,n} = \overline{\varepsilon}_{Fn-1,n} \qquad \{1.13\}$$

$$\tilde{\varepsilon}_{Fn-1,n}(t) = \frac{\tilde{F}_{n-1,n}(t)}{\overline{A}_e\overline{E}_{n-1,n}} \qquad \{1.14\}$$

hold. It is seen in {1.10} that the amplitude of $\tilde{z}_{TEn-1}$ is proportional to the difference of strains $\left(\overline{\varepsilon}_{n-1,n} - \overline{\varepsilon}_{n-2,n-1}\right)$ which virtually could not be measured with a real printing press. A new result is that this difference can be expressed through the so-called “advance” (also denoted as “lead” or “gain” or “speed draw”)

$$\overline{W}_{n,n-1} = \frac{\overline{v}_{cn}}{\overline{v}_{cn-1}} - 1 = \overline{\varepsilon}_{n-1,n} - \overline{\varepsilon}_{n-2,n-1} \qquad \{1.15\}$$

which is precisely known by the preset value of the master control console. These equations are applied to the three roller system of Fig. 3a, giving

$$\tilde{\varepsilon}_{12} = \frac{1}{1+T_{12}s}\left(\tilde{\varepsilon}_{01} + \left(\overline{\varepsilon}_{12} - \overline{\varepsilon}_{01}\right)\tilde{z}_{TE1} + \frac{\tilde{v}_{c2} - \tilde{v}_{c1}}{\overline{v}}\right) \qquad \{1.16\}$$

$$\tilde{\varepsilon}_{23} = \frac{1}{1+T_{23}s}\left(\tilde{\varepsilon}_{12} + \left(\overline{\varepsilon}_{23} - \overline{\varepsilon}_{12}\right)\tilde{z}_{TE1}e^{-T_{12}s} + \frac{\tilde{v}_{c3} - \tilde{v}_{c2}}{\overline{v}}\right) \qquad \{1.17\}$$

Inserting {1.16} into {1.17} yields

$$\tilde{\varepsilon}_{23} = \frac{1}{1+T_{23}s}\left[\begin{array}{l} \dfrac{1}{1+T_{12}s}\left(\tilde{\varepsilon}_{01} - \dfrac{\tilde{v}_{c1}}{\overline{v}}\right) + \dfrac{\tilde{v}_{c3}}{\overline{v}} - \dfrac{T_{12}s}{1+T_{12}s}\dfrac{\tilde{v}_{c2}}{\overline{v}} \\ + \left(\dfrac{1}{1+T_{12}s}\left(\overline{\varepsilon}_{12} - \overline{\varepsilon}_{01}\right) + \left(\overline{\varepsilon}_{23} - \overline{\varepsilon}_{12}\right)e^{-T_{12}s}\right)\tilde{z}_{TE1} \end{array}\right] \qquad \{1.18\}$$

Fig. 3b shows the resultant block diagram which illustrates that the transport disturbance $\tilde{z}_{TE1}$ triggers a transient at every nip.

In order to discuss some fundamental properties of the web dynamics in the ideal system with micro slip, step responses are calculated.

a) If $\tilde{z}_{TE1} = \tilde{v}_{c1} = \tilde{v}_{c2} = \tilde{v}_{c3} \equiv 0$ is assumed

$$\tilde{\varepsilon}_{12} = \frac{1}{1+T_{12}s}\tilde{\varepsilon}_{01} \qquad \{1.19\}$$

and

$$\tilde{\varepsilon}_{23} = \frac{1}{(1+T_{12}s)(1+T_{23}s)}\tilde{\varepsilon}_{01} \qquad \{1.20\}$$

result. Applying a step function to $\tilde{\varepsilon}_{01}$ the steady-state value can be calculated as

$$\lim_{t\to\infty}\tilde{\varepsilon}_{23} = \tilde{\varepsilon}_{23\infty} = \lim_{s\to 0}\frac{1}{\left(1+T_{12}s\right)\left(1+T_{23}s\right)}\hat{\varepsilon}_{01} = \hat{\varepsilon}_{01} = \tilde{\varepsilon}_{12\infty} \qquad \{1.21\}$$

The full magnitude of strain

$$\tilde{\varepsilon}_{12\infty} = \tilde{\varepsilon}_{23\infty} = \hat{\varepsilon}_{01} = \hat{F}_{01} / \overline{A}_e\overline{E}_{01} = \tilde{F}_{12} / \overline{A}_e\overline{E}_{12} = \tilde{F}_{23} / \overline{A}_e\overline{E}_{23} \qquad \{1.22\}$$

arrives at roller 3. If $\overline{E}_{12} = \overline{E}_{23} = \overline{E}_{01}$ holds $\tilde{F}_{12\infty} = \tilde{F}_{23\infty} = \hat{F}_{01}$ results.

b) If $\tilde{z}_{TE1} = \tilde{\varepsilon}_{01} = \tilde{v}_{c1} = \tilde{v}_{c3} \equiv 0$ is assumed the equations

$$\tilde{\varepsilon}_{12} = \frac{1}{1+T_{12}s}\frac{\tilde{v}_{c2}}{\overline{v}} \qquad \{1.23\}$$

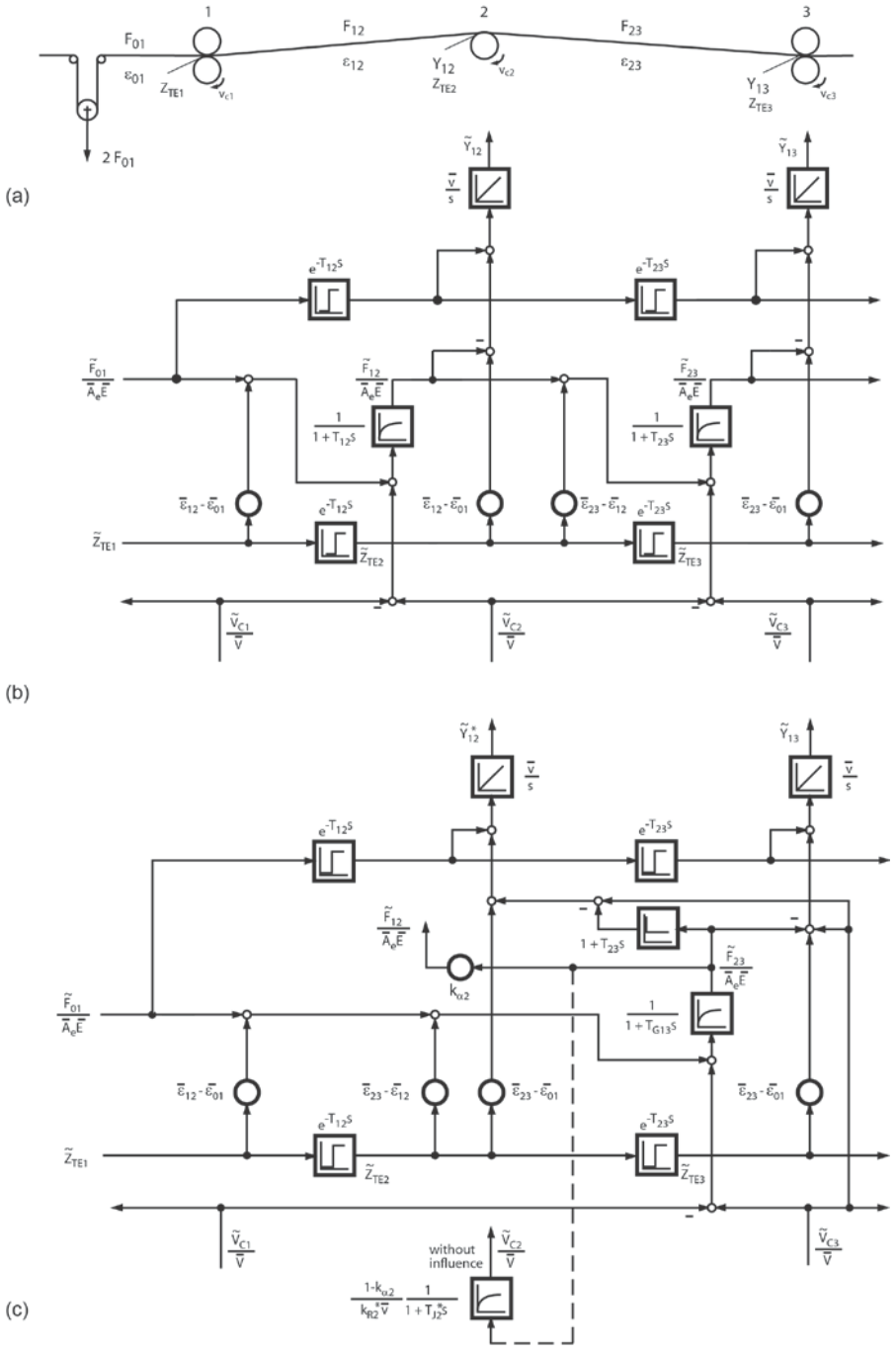

Figure 3 – Three-roller system (a) and block diagrams representing micro slip (b) and macro slip (c); $\bar{E}_{01} = \bar{E}_{12} = \bar{E}_{23} = \bar{E}$

and

$$\tilde{\varepsilon}_{23} = \frac{T_{12}s}{1+T_{12}s}\frac{1}{1+T_{23}s}\frac{\tilde{v}_{c2}}{\overline{v}} \qquad \{1.24\}$$

are obtained. Applying a step function to $\tilde{v}_{c2}$, strain $\tilde{\varepsilon}_{12}$ reaches the steady-state value

$$\tilde{\varepsilon}_{12\infty} = \frac{\hat{v}_{c2}}{\overline{v}} \qquad \{1.25\}$$

whereas $\tilde{\varepsilon}_{23}$ cannot be changed permanently,

$$\tilde{\varepsilon}_{23\infty} = 0 \qquad \{1.26\}$$

The deflection of strain $\tilde{\varepsilon}_{23}$ due to $\hat{v}_{c2}$ is "self compensating".

c) If $\tilde{\varepsilon}_{01} = \tilde{v}_{c1} = \tilde{v}_{c2} = \tilde{v}_{c3} \equiv 0$ and $\tilde{z}_{TE1} \neq 0$ is assumed

$$\tilde{\varepsilon}_{12} = \frac{1}{1+T_{12}s}\left(\overline{\varepsilon}_{12} - \overline{\varepsilon}_{01}\right)\tilde{z}_{TE1} \qquad \{1.27\}$$

and

$$\tilde{\varepsilon}_{23} = \frac{1}{1+T_{23}s}\left[\frac{1}{1+T_{12}s}\left(\overline{\varepsilon}_{12} - \overline{\varepsilon}_{01}\right) + \left(\overline{\varepsilon}_{23} - \overline{\varepsilon}_{12}\right)e^{-T_{12}s}\right]\tilde{z}_{TE1} \qquad \{1.28\}$$

result. Applying a step function to $\tilde{z}_{TE1}$ the steady-state values

$$\tilde{\varepsilon}_{12\infty} = \left(\overline{\varepsilon}_{12} - \overline{\varepsilon}_{01}\right)\hat{z}_{TE1} \qquad \{1.29\}$$

and

$$\tilde{\varepsilon}_{23\infty} = \left(\overline{\varepsilon}_{23} - \overline{\varepsilon}_{01}\right)\hat{z}_{TE1} \qquad \{1.30\}$$

are reached (c.f. [6]).

In order to confirm these theoretical results and to compare them to the case of macro slip (c.f. Section 6), a step change of F_{01} has been simulated and measured with a standard commercial offset press of type ROTOMAN manufactured by MAN Roland in Augsburg (Germany). The three roller system of Fig. 3 has been realized through the units 5, 6 und 7 of Fig. 1. Rollers 5 and 7 more or less behave as ideal nips with micro slip, whereas roller 6 could be varied between micro slip and macro slip with the help of the speed controlled drive [11]. The simulated curves of Fig. 4b represent the theoretical performance: The change of tensile force $\hat{F}_{01}$ spreads out along the press with $\tilde{F}_{45\infty} = \tilde{F}_{56\infty} = \tilde{F}_{67\infty} = \hat{F}_{01}$ because $\overline{E}_{n-1,n} = \overline{E}_{01}$ was assumed. The curves are continuously

smoothed. The measured curves of Fig. 4a are in surprisingly good accordance with the simulated ones. Similar good results have been measured in the case of step changes of $\tilde{v}_{c2}$. Step changes of the area of cross section have been experimentally realized by pasting a web of small width to a web with big width and transporting it through the press. The correctness of {1.29} and {1.30} could be confirmed qualitatively.

The register errors of Fig. 4c and 4d will be discussed in Sections 3 and 4.

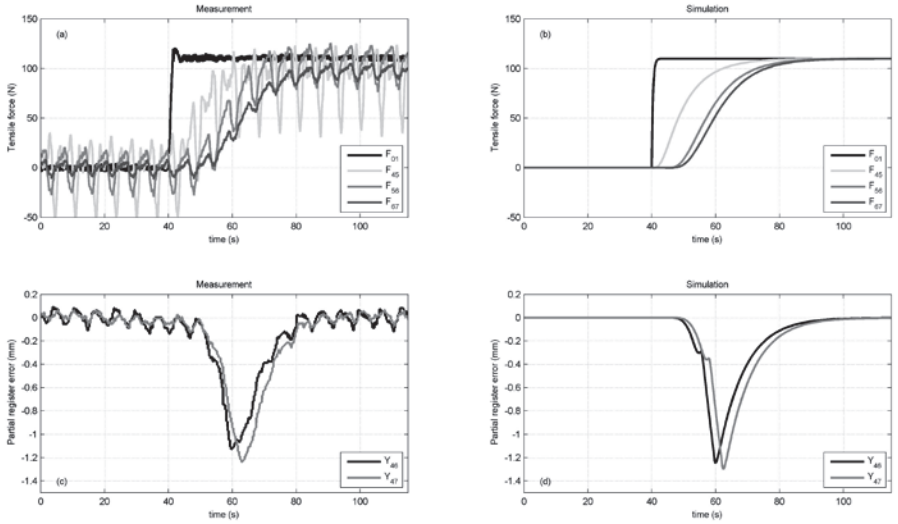

Fig. 4 – Step responses with micro-slip. Left: Measurement. Right: Simulation. Web forces (a), (b) and partial register errors (b), (c), (asterisks not printed)

2. REGISTER ERRORS AND DOUBLING

Terminology

A printed product has to satisfy certain quality requirements which are very high in the case of heat-set commercial presses. The so-called color register error must be kept within a tolerance band of $\pm 0.01\ mm$, the cutting register within $\pm 0.4\ mm$. The color register error is the distance of two different-colored printed points which represent the same original point. The cutting register error is the distance of the actual cut with respect to the reference cut.

The doubling (or "ghosting") error is double printing in the same color due to color splitting. Often oscillations of the printing cylinders induce doubling which affects the color tone. Though doubling mainly occurred in presses with long mechanical line shafts, it is occasionally also found in modern machines with electronic line shafts. Doubling can occur either within a printing unit or between two printing units. Only the latter is explained here using Fig. 5, c.f. [12].

Mathematical Model

An offset printing unit consists of a plate cylinder and a blanket cylinder which are coupled mechanically. The image on the plate cylinder (PZ) is transferred to blanket cylinder (GZ) which prints the image on the paper. In Fig. 5 the points 1a, 1b (e.g. cyan) and 2a (e.g. magenta) represent the same point of the image to be printed. Point 1a is

printed at time $t = t_{p1a}$ and transported with the running web (Fig. 5a). After half a turn of the rollers, point 1b is transferred from PZ 1 to GZ 1 and half a turn later, at $t = t_{p1b}$, printed onto the paper (Fig. 5b). When 2a is printed by unit 2 at $t = t_{p2a}$, point 1a should

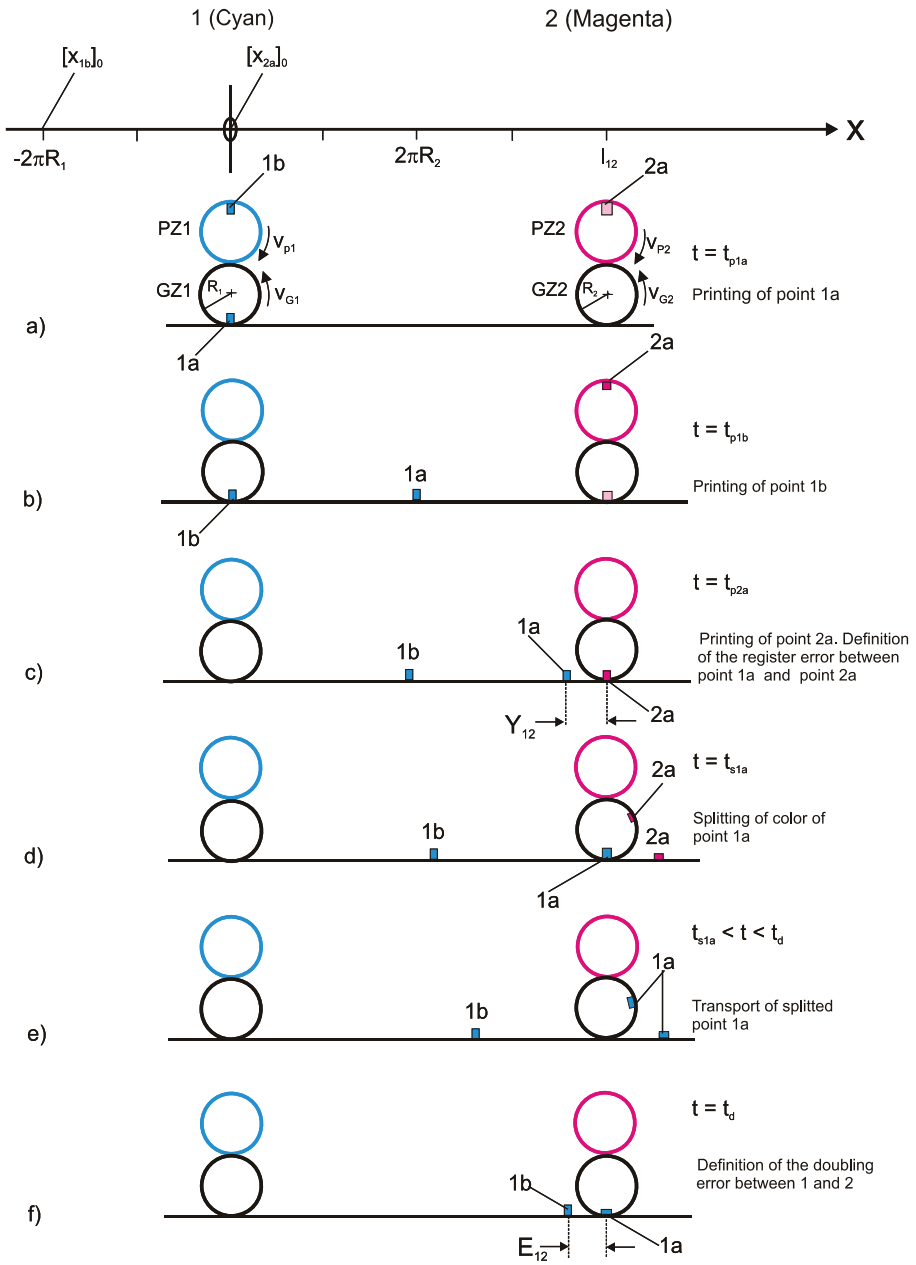

Figure 5 – Color register error Y_{12} and doubling error E_{12} between printing unit 1 and 2

have reached the position $x = l_{12}$. But due to disturbances in web strain a difference between both points may exist. This is the color register error Y_{12} (Fig. 5c). When at time $t = t_{s1a}$ point 1a reaches the nip of unit 2, it transfers color to the blanket cylinder by ink splitting. This "ghost point" is transported with GZ 2 and is printed a second time at $t = t_d$. At this point of time point 1b should have reached GZ 2. But a distance E_{12}, denoted as doubling error (Fig. 6f), may exist due to disturbances in the web. An important result is: Variations of web strain lead to color register errors and additionally splitting of color causes doubling errors. The essential linearized model equations, c.f. [6], [7], and [12], are

$$\tilde{Y}_{12} = \frac{\overline{v}}{s}\left(-\tilde{\varepsilon}_{E2} + e^{-T_{12}s}\tilde{\varepsilon}_{E1}\right) \qquad \{2.1\}$$

and

$$\tilde{E}_{12}(s) = \frac{\overline{v}}{s}(1-e^{-T_u s})[-\tilde{\varepsilon}_{E2}(s) + e^{-T_{12}s}\tilde{\varepsilon}_{E1}(s)] = (1-e^{-T_u s})\tilde{Y}_{12}(s) \qquad \{2.2\}$$

with

$$T_U = 2\pi / \overline{\omega} \qquad \{2.3\}$$

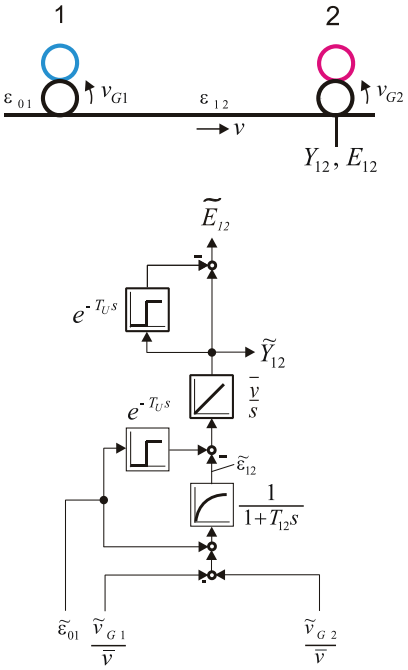

Figure 6 – Block diagram of register error $\tilde{Y}_{12}$ and doubling error $\tilde{E}_{12}$ $\overline{\omega}$ being the steady-state angular velocity of the cylinders. If the strain ε does not depend on x, the strain $\tilde{\varepsilon}_{En}$ at the input of a roller n can be replaced by $\tilde{\varepsilon}_{n-1,n}$ in both

equations, $\tilde{\varepsilon}_{n-1,n}$ being the strain in the upstream "free web" section. In Fig. 6 the block diagram is shown. In order to confirm the theory, measurements have been carried out by applying an aperiodic displacement Δx to printing unit 2 (see Fig. 1), thus artificially generating a register error Y_{12} and a doubling error E_{12}. A comparison of the measured to the simulated curves (see Fig. 7) proves the correctness of the theory with surprising accuracy.

Often doubling is induced through periodic signals, e. g. oscillations of the cylinders. The mathematical model clearly shows that oscillation frequencies f_o which are whole-number multiples of the rotational frequency, i. e.

$$f_o = k f_u = k / T_u = k\bar{\omega}/(2\pi) \text{ with } k = 1, 2, \ldots, n, \qquad \{2.4\}$$

cannot induce doubling errors due to the time delay block at the top end of Fig. 6 and the sign subtraction.

Equation (2.1) can be extended to the color register error between nip 1 and any nip n to give

$$\tilde{Y}_{1n} = \frac{\bar{v}}{s}\left(-\tilde{\varepsilon}_{En} + e^{-T_{1n}s}\tilde{\varepsilon}_{E1}\right) \qquad \{2.5\}$$

The total cutting register error principally satisfies the same equation. Generalizing (2.2) yields correspondingly

$$\tilde{E}_{1n}(s) = (1 - e^{-T_u s})\tilde{Y}_{1n}(s) \qquad \{2.6\}$$

Furthermore, inserting {1.11} and {1.14} into (2.5) yields

$$\begin{aligned}\tilde{Y}_{1n}(s) &= \frac{\bar{v}}{s}\left[-\tilde{\varepsilon}_{Fn-1,n}(s) + e^{-T_{1n}s}\tilde{\varepsilon}_{F01}(s) + \left(\bar{\varepsilon}_{n-1,n} - \bar{\varepsilon}_{01}\right)\tilde{z}_{TEn}(s)\right] \\ &= \frac{\bar{v}}{s}\left[-\frac{\tilde{F}_{n-1,n}(s)}{\bar{A}_e\bar{E}_{n-1,n}} + e^{-T_{1n}s}\frac{\tilde{F}_{01}(s)}{\bar{A}_e\bar{E}_{01}} + \left(\bar{\varepsilon}_{n-1,n} - \bar{\varepsilon}_{01}\right)e^{-T_{1n}s}\tilde{z}_{TE1}(s)\right]\end{aligned} \qquad \{2.7\}$$

3. PARTIAL REGISTER ERRORS

Statement of the Problem

In a printing press the paper web is exposed to numerous periodic and non-periodic disturbances. The paper absorbs water and color in the printing nips and expands. In the dryer the web contracts again, and it will experience further dimensional changes on the rollers of the chilling unit due to cooling. These and other various influences lead to increasing and decreasing position changes of the printed images relatively to the position of the blade of the rotating cutting cylinder at the end of the press (nip 8 on Fig. 1). At this point a significant "total" cutting register error (TCRE) occurs, as the paper adds up the many "partial" cutting register errors (PCRE) during its travel through the printing press.

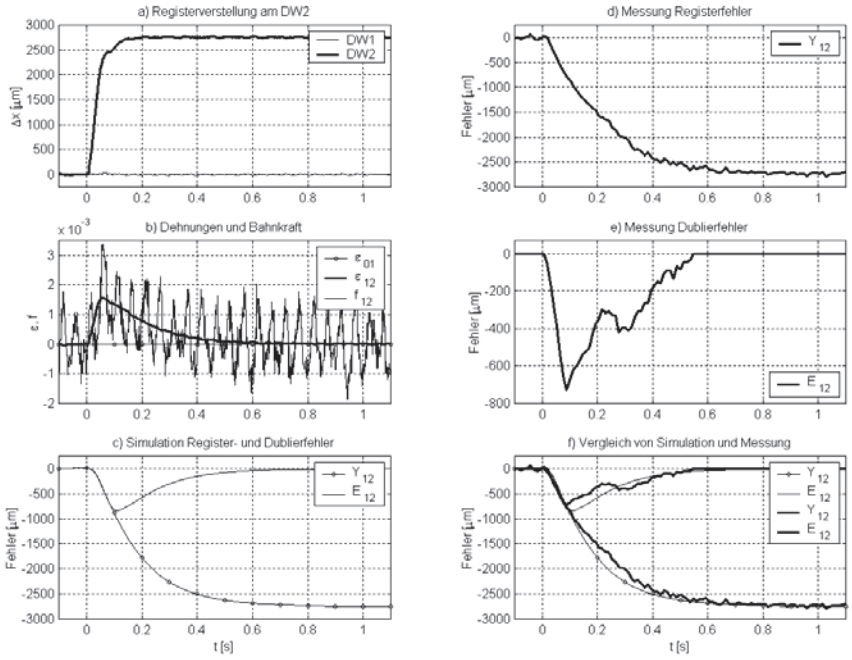

a) Register displacement (μm) of DW 2, b) strain and force, c) simulation of register and doubling error (μm), d) measured register error (μm), e) measured doubling error (μm), d) comparison of simulation and measurement

Figure 7 – Doubling between printing units 1 and 2 due to displacement of printing unit (DW) 2

It is advantageous, therefore, to control one or even several PCREs before a big TCRE at the cutting cylinder has been built up. Optical sensors can be provided in certain sections of the printing press to detect these errors (e.g. at nip 3 in Fig. 15a). A mathematical model of the PCRE has been derived, c.f. [14], which has led to a completely new control scheme which considerably reduces the rate of waste paper in heat set commercial presses for illustration printing and for letter press printing, [14] and [15].

Mathematical Model

In Fig. 8a nip 1 is a printing unit whereas nip 2 and 3 are assumed to be electrically driven, non-printing drawing rollers. Nip 1 prints point 1a, which may represent the cutting line between two images, at time $t = t_{P1a}$. In steady-state this point passes the position $x = l_{1M}$ of sensor S1 at time $t = \overline{t}_{B1a}$ and is measured by S1. In transient motion, however, point 1 would not reach this position: A PCRE Y^*_{M12} occurs in section 1-2 (Fig. 8b) which can be calculated by an algorithm implemented within the sensor. After having

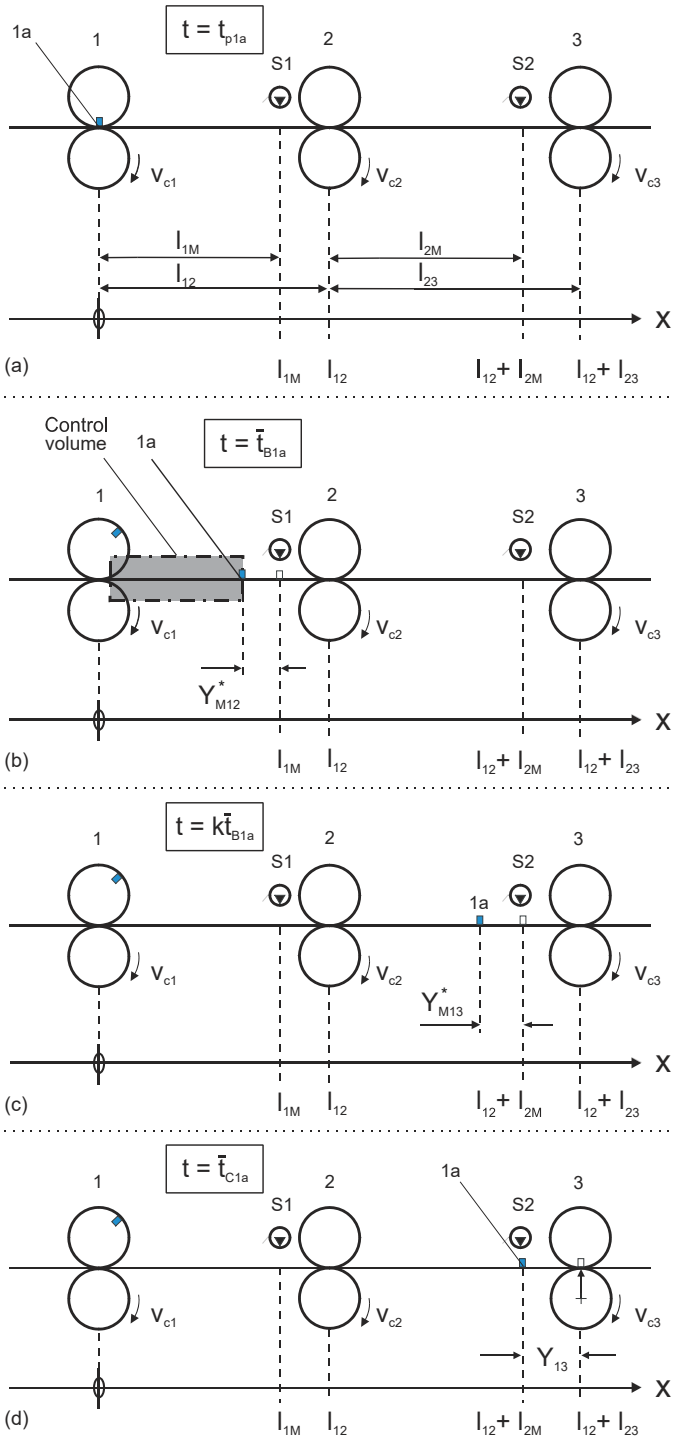

Figure 8 – Partial cutting register errors

passed nip 1 the PCRE has changed to be Y^*_{M13} at the position $x = l_{12} + l_{2M}$ (Fig. 8c) and is measured by the sensor S2 at time $t = k\overline{t}_{B1a}$ (with k accounting for the position of sensor S2). If we now assume that nip 3 in Fig. 8d is a cutting cylinder the TCRE Y_{13} would occur at $t = \overline{t}_{C1a}$.

If not only a singular point is considered, but all successive points that are printed by nip 1, the PCRE at a position $x = l_{i-1,i} + l_{iM}$ becomes a continuous function of time, For details of mathematics see [12], [13], and [14]. If the sensor is mounted next to the nip 2 the PCRE $\tilde{Y}^*_{12}$ (index M dropped, c.f. [14]) can be calculated to be

$$\tilde{Y}^*_{12} = \frac{\overline{v}}{s}\left(-\tilde{\varepsilon}_{E2} + e^{-T_{12}s}\tilde{\varepsilon}_{E1} + \frac{\tilde{v}_{c2}}{\overline{v}} \right) \qquad \{3.1\}$$

Generalizing this equation yields the PCRE measured at a non-printing nip n, when the reference nip is number 1:

$$\tilde{Y}^*_{1n} = \frac{\overline{v}}{s}\left(-\tilde{\varepsilon}_{En} + e^{-T_{1n}s}\tilde{\varepsilon}_{E1} + \frac{\tilde{v}_{cn}}{\overline{v}} \right) \qquad \{3.2\}$$

The Index 1 can be substituted by the index $p < n$ for any upstream nip p

$$\tilde{Y}^*_{pn} = \frac{\overline{v}}{s}\left(-\tilde{\varepsilon}_{En} + e^{-T_{pn}s}\tilde{\varepsilon}_{Ep} + \frac{\tilde{v}_{cn}}{\overline{v}} \right) \qquad \{3.3\}$$

with the transport time T_{pn} from nip p to nip n. [1] If {1.9}, {1.10}, and {1.11} are inserted into {3.2} one receives

$$\begin{aligned} \tilde{Y}^*_{1n}(s) &= \frac{\overline{v}}{s}\left[-\tilde{\varepsilon}_{Fn-1,n}(s) + e^{-T_{1n}s}\tilde{\varepsilon}_{F01}(s) + \left(\overline{\varepsilon}_{n-1,n} - \overline{\varepsilon}_{01}\right)\tilde{z}_{TEn}(s) + \frac{\tilde{v}_{cn}(s)}{\overline{v}} \right] \\ &= \frac{\overline{v}}{s}\left[\begin{array}{l} -\dfrac{\tilde{F}_{n-1,n}(s)}{\overline{A}_e\overline{E}_{n-1,n}} + e^{-T_{1n}s}\dfrac{\tilde{F}_{01}(s)}{\overline{A}_e\overline{E}_{01}} \\ +\left(\overline{\varepsilon}_{n-1,n} - \overline{\varepsilon}_{01}\right)e^{-T_{1n}s}\tilde{z}_{TE1}(s) + \dfrac{\tilde{v}_{cn}(s)}{\overline{v}} \end{array} \right] \end{aligned} \qquad \{3.4\}$$

If index 1 is substituted by p it follows

---

[1] The indices of {3.3} are simpler than those used in [15] and [16] which read $\tilde{Y}^*_{k-q,k}(s) = \left[-\tilde{\varepsilon}_{Ek}(s) + \tilde{\varepsilon}_{E,k-q}(s)e^{-T_{k-q,k}s} + \tilde{v}_{ck}(s)/\overline{v} \right]\overline{v}/s$. In this notation k denotes the nip where $\tilde{Y}^*_{k-q,k}$ is measured and $k-q$ denotes the reference nip.

$$\tilde{Y}^{*}_{pn}(s)=\frac{\overline{v}}{s}\left[-\tilde{\varepsilon}_{Fn-1,n}(s)+e^{-T_{pn}s}\tilde{\varepsilon}_{Fp-1,p}(s)+\left(\overline{\varepsilon}_{n-1,n}-\overline{\varepsilon}_{p-1,p}\right)\tilde{z}_{TEn}(s)+\frac{\tilde{v}_{cn}(s)}{\overline{v}}\right] \qquad \{3.5\}$$

Choosing e.g. $k=7$ and $p=4$ (c.f. Fig. 10 and Fig. 11) the formula

$$\tilde{Y}^{*}_{47}(s)=\frac{\overline{v}}{s}\left[-\tilde{\varepsilon}_{F67}(s)+e^{-T_{47}s}\tilde{\varepsilon}_{F34}(s)+\left(\overline{\varepsilon}_{47}-\overline{\varepsilon}_{34}\right)\tilde{z}_{TE7}(s)+\frac{\tilde{v}_{c7}(s)}{\overline{v}}\right] \qquad \{3.6\}$$

is received for the PCRE between the reference nip 4 and the sensor at nip 7 (c.f. Fig. 1). The transport disturbance $\tilde{z}_{TEn}$ and the properties of the register errors will be discussed in Section 4.

By introducing the PCRE into the mathematical model a new cutting register control strategy can be developed: The PRCE $\tilde{Y}^{*}_{pn}$ is measured at any appropriate nip n and is compensated for with the help of its velocity $\tilde{v}_{cn}$. This strategy can be combined with a control of the TCRE at the cutting cylinder, thus achieving a considerable reduction of paper waste [17].

4. COMPARISON OF TOTAL AND PARTIAL CUTTING REGISTER ERRORS

In order to compare the partial and total cutting register errors, step functions are applied to ε_{01} and v_{c2} in the system of Fig. 1 and Fig. 3b respectively. The step responses and the steady-state values of the TCRE and the PCRE are discussed.

Total Cutting Register Error

The TCRE $\tilde{Y}_{13}$ is calculated assuming a change of $\tilde{v}_{c2}$. If position independent strains are assumed equation {2.5} reads

$$\tilde{Y}_{13}=\frac{\overline{v}}{s}\left(-\tilde{\varepsilon}_{23}+\tilde{\varepsilon}_{01}e^{-T_{13}s}\right) \qquad \{4.1\}$$

In order to calculate the TCRE, {1.18} with $\tilde{z}_{TE1}\equiv 0$ is inserted into {4.1}, giving

$$\tilde{Y}_{13}=\frac{\overline{v}}{s}\left\{-\frac{1}{1+T_{23}s}\left[\left(\frac{1}{1+T_{12}s}-e^{-T_{13}s}\right)\tilde{\varepsilon}_{01}-\frac{1}{1+T_{12}s}\frac{\tilde{v}_{c1}}{\overline{v}}-\frac{T_{12}s}{1+T_{12}s}\frac{\tilde{v}_{c2}}{\overline{v}}+\frac{\tilde{v}_{c3}}{\overline{v}}\right]\right\} \qquad \{4.2\}$$

Applying the step function to $\tilde{\varepsilon}_{01}$ yields the steady-state value

$$\lim_{t\to\infty}\tilde{Y}_{13}=\tilde{Y}_{13\infty}=\lim_{s\to 0}\frac{\overline{v}}{s}\frac{1}{1+T_{23}s}\left(-\frac{1}{1+T_{12}s}+e^{-T_{13}s}\right)\hat{\varepsilon}_{01}=0 \qquad \{4.3\}$$

The TCRE is self compensating with respect to $\tilde{\varepsilon}_{01}$.

If the circumferential speed v_{c2} of the non-printing roller 2 changes {4.2} gives

$$\tilde{Y}_{13} = \frac{1}{1+T_{23}s}\frac{\overline{v}T_{12}}{1+T_{12}s}\frac{\tilde{v}_{c2}}{\overline{v}} = \frac{1}{1+T_{23}s}\frac{l_{12}}{1+T_{12}s}\frac{\tilde{v}_{c2}}{\overline{v}} \qquad \{4.4\}$$

Applying a step function to v_{c2} a steady-state TCRE

$$\lim_{t\to\infty}\tilde{Y}_{13} = \tilde{Y}_{13\infty} = \lim_{s\to 0}\frac{\overline{v}}{s}\frac{1}{1+T_{23}s}\frac{T_{12}s}{1+T_{12}s}\frac{\hat{v}_{c2}}{\overline{v}} = \lim_{s\to 0}\frac{1}{1+T_{23}s}\frac{l_{12}}{1+T_{12}s}\frac{\hat{v}_{c2}}{\overline{v}} = l_{12}\frac{\hat{v}_{c2}}{\overline{v}} \qquad \{4.5\}$$

is generated, which is proportional to the relative step magnitude $\hat{v}_{c2}/\overline{v}$ and the length of the free web. In contrast, step functions of v_{c1} or v_{c3} lead to infinite total cutting register errors.

Partial Cutting Register Error

For the purpose of comparison of the PCRE to the TCRE, $\tilde{Y}_{12}^{*}$ is calculated now from {3.1} which reads, if position independent strains are assumed,

$$\tilde{Y}_{12}^{*} = \frac{\overline{v}}{s}\left(-\tilde{\varepsilon}_{12} + \tilde{\varepsilon}_{01}e^{-T_{13}s} + \frac{\tilde{v}_{c2}}{\overline{v}}\right) \qquad \{4.6\}$$

Inserting of {1.17} with $\tilde{z}_{TE1} \equiv 0$ gives

$$\tilde{Y}_{12}^{*} = \frac{\overline{v}}{s}\left[-\frac{1}{1+T_{12}s}\left(\tilde{\varepsilon}_{01} + \frac{\tilde{v}_{c2}-\tilde{v}_{c1}}{\overline{v}}\right) + \tilde{\varepsilon}_{01}e^{-T_{12}s} + \frac{\tilde{v}_{c2}}{\overline{v}}\right] \qquad \{4.7\}$$

and it follows

$$\tilde{Y}_{12}^{*} = \frac{\overline{v}}{s}\left[\left(-\frac{1}{1+T_{12}s} + e^{-T_{12}s}\right)\tilde{\varepsilon}_{01} - \frac{1}{1+T_{12}s}\frac{\tilde{v}_{c1}}{\overline{v}} + \frac{T_{12}s}{1+T_{12}s}\frac{\tilde{v}_{c2}}{\overline{v}}\right] \qquad \{4.8\}$$

A step of $\tilde{\varepsilon}_{01}$ results in self compensation of $\tilde{Y}_{12\infty}^{*}$,

$$\tilde{Y}_{12\infty}^{*} = 0 \qquad \{4.9\}$$

This is confirmed by Fig. 4c and 4d. If v_{c2} changes the relationship

$$\boxed{\tilde{Y}_{12}^{*} = \frac{\overline{v}T_{12}}{1+T_{12}s}\frac{\tilde{v}_{c2}}{\overline{v}} = \frac{l_{12}}{1+T_{12}s}\frac{\tilde{v}_{c2}}{\overline{v}}} \qquad \{4.10\}$$

is obtained. This equation is exactly part of {4.4}! Inserting {4.10} into {4.4} gives

$$\boxed{\tilde{Y}_{13} = \frac{1}{1+T_{23}s}\tilde{Y}_{12}^{*}} \qquad \{4.11\}$$

It is evident now that the term $\tilde{v}_{ck}/\overline{v}$ which has been found in section 3 for the PCRE $\tilde{Y}_{1k}^{*}$ provides for a transformation of a printing nip k into a non-printing nip. Hence, {4.10} proves the correctness of the mathematical model of the partial cutting register error derived in Section 3. A change of v_{c2} generates a PCRE $\tilde{Y}_{12}^{*}$ which can be measured with a sensor at the input of the non-printing nip 2 in Fig. 3b (or nip 6 in Fig. 1). This error is transported to the cutting cylinder 3, and is simultaneously being filtered with T_{23}.

Equation {4.10} has become the basic relationship for the design of the control of a PCRE $\tilde{Y}_{1k}^{*}$ with the speed of the roller k, c.f. [17] and Section 8. Applying a step function to $\tilde{v}_{c2}$ the steady-state PCRE

$$\tilde{Y}_{12\infty}^{*} = l_{12}\frac{\hat{v}_{c2}}{\overline{v}} \qquad \{4.12\}$$

is reached. This equation shows that $\tilde{Y}_{12\infty}^{*}$ is a linear function of $\hat{v}_{c2}/\overline{v}$ with slope l_{12}. A measured nonlinear characteristic indicates macro slip (c.f. section 6) or partial slip (c.f. section 7) of roller 2.

5. RECONTRUCTION OF TRANSPORT DISTURBANCES

General Relationships

Though transport disturbances are very important factors in printing presses, because they can induce color and cutting register errors of high magnitude with high paper waste, nobody has ever seen one. They are not directly measurable. The idea was, therefore, to reconstruct it with the help of the partial register error.

A general equation for the reconstruction of $\tilde{z}_{TEn}$ can be found by rearranging {3.4} to obtain

$$\tilde{z}_{TEn} = e^{-T_{1n}s}\tilde{z}_{TE1} = \frac{1}{\overline{W}_{n1}}\left(\frac{s}{\overline{v}}\tilde{Y}_{1n}^{*} + \frac{\tilde{F}_{n-1,n}}{\overline{A}_e\overline{E}_{n-1,n}} - e^{-T_{1n}s}\frac{\tilde{F}_{01}}{\overline{A}_e\overline{E}_{01}} - \frac{\tilde{v}_{cn}}{\overline{v}}\right) \qquad \{5.1\}$$

with

$$\tilde{z}_{TEn} = \frac{\tilde{A}_{eEn}}{\overline{A}_e} + \frac{\tilde{E}_{En}}{\overline{E}_{En}} \qquad \{5.2\}$$

and

$$\overline{W}_{n1} = \frac{\overline{v}_{cn}}{\overline{v}_{c1}} - 1 = \overline{\varepsilon}_{n-1,n} - \overline{\varepsilon}_{01} \qquad \{5.3\}$$

As an example, by choosing $\tilde{z}_{TEn2}$ in Fig. 3b we have

$$\tilde{z}_{TE2} = e^{-T_{12}s}\tilde{z}_{TE1} = \frac{1}{\overline{W}_{21}}\left(\frac{s}{\overline{v}}\tilde{Y}_{12}^{*} + \frac{\tilde{F}_{12}}{\overline{A}_e\overline{E}_{12}} - e^{-T_{12}s}\frac{\tilde{F}_{01}}{\overline{A}_e\overline{E}_{01}} - \frac{\tilde{v}_{c2}}{\overline{v}}\right) \qquad \{5.4\}$$

with the time constant

$$T_{12} = \frac{l_{12}}{\overline{v}} \qquad \{5.5\}$$

The general reconstruction equations {5.1} or {5.4} require 4 variables and 5 steady-state constants to be known. Often F_{01} and v_{c2} can be kept constant, i.e. $\tilde{F}_{01} \approx 0$ and $\tilde{v}_{c2} \equiv 0$. Then

$$\tilde{z}_{TE2} = e^{-T_{12}s}\tilde{z}_{TE1} = \frac{1}{\overline{W}_{21}}\left(\frac{s}{\overline{v}}\tilde{Y}_{12}^{*} + \frac{\tilde{F}_{12}}{\overline{A}_e\overline{E}_{12}}\right) = \frac{1}{\overline{W}_{21}}\left(\frac{s}{\overline{v}}\tilde{Y}_{12}^{*} + \tilde{\varepsilon}_{F12}\right) \qquad \{5.6\}$$

follows. As $s\tilde{Y}_{12}^{*}$ is a differentiation, the measured signal $\tilde{Y}_{12}^{*}$ has to be filtered. The mean value of the transport speed of the web is well-known from the electronic line shaft, $\overline{W}_{21}$ is precisely known from the reference values of the drives. The cross section $\overline{A}_e$ of the web can be calculated from the width and the caliper of the web. The web tension F_{12} can be measured with a tension sensing roller with satisfying accuracy. Young's modulus in a web span can be identified online by applying appropriate test functions, see e.g. [18].

Experimental Results

The curves on Fig. 9 have been measured with a newspaper printing press [10]. The reel change occurs at $t = 0$ as can be seen from the tension F_{12}. If $\tilde{z}_{TE1}$ arrives at nip 1 with a step function at $t = 0$, $\tilde{z}_{TE2}(t < T_{12}) \equiv 0$ is theoretically required for the reconstructed signal. This behaviour is approximately observable on Fig 9 (right side). Apparently $\tilde{z}_{TE2}$ rises similar to a step function (see left side on Fig. 9) at $t \approx T_{12}$, reaches a maximum value $\tilde{z}_{TE2,\max} \approx \tilde{E}_{12\max} / \overline{E}_{12} \approx 1.2$ at $t \approx 4T_{12}$ and declines slowly to a constant new quasi steady-state value. The measurement was finished at $t = 180\ ms$.

Many useful applications of he reconstructed transport disturbance can be suggested. On the one hand one gets a deeper understanding of the properties of the web in the reel and in the spans of a press, on the other hand, feed-forward controls for reducing the total cutting register error are possible.

PART 2 ROLLERS WITH MACRO SLIP AND PARTIAL SLIP

6. ROLLERS WITH MACRO SLIP

In this section total slipping of the web over the roller surface is dealt with which often occurs in web handling systems.

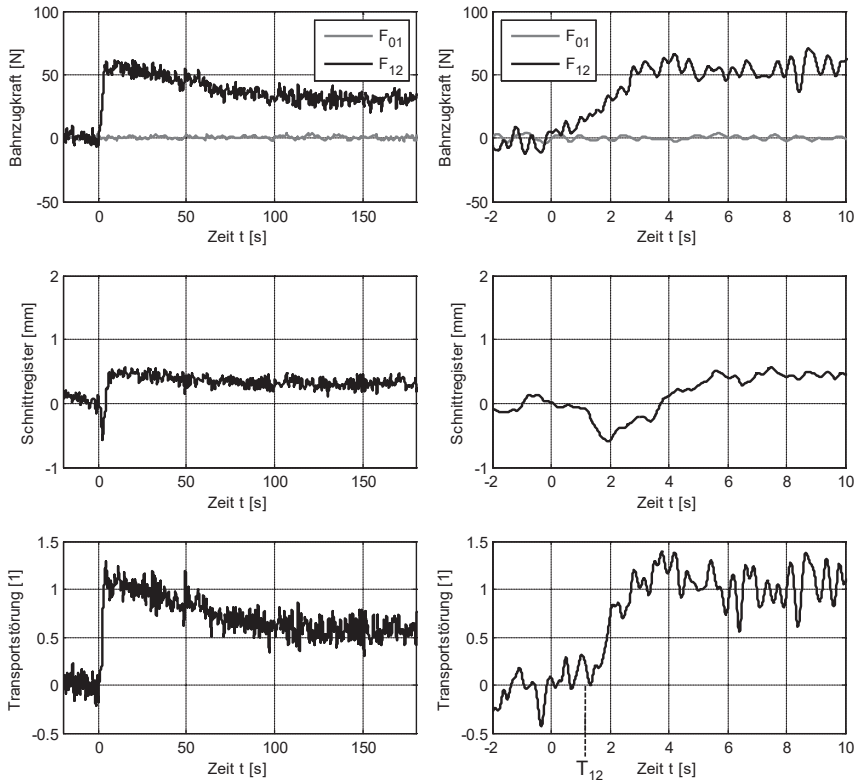

Bahnzugkraft = tensile force $\tilde{F}_{12}$ ($\tilde{F}_{01} \approx 0$)
Schnittregister = partial cutting register error $\tilde{Y}_{12}^{*}$
Transportstörung = transport disturbance $\tilde{z}_{TE2}$
Zeit = time t

Figure 9 – Reconstruction of the transport disturbance $\tilde{z}_{TE2}$ with the help of partial register error $\tilde{Y}_{12}^{*}$ und force $\tilde{F}_{12}$ (measurement at $\overline{v} = 30.000\ Ex/h = 9.6\ m/s$)

For explanation, steady-state motion with $\overline{F}_{23} > \overline{F}_{12}$ is assumed for a moment. If $\overline{F}_{23}$ is increased and reaches the value of $\overline{F}_{23} / \overline{F}_{12} = \exp(\mu\alpha_2)$ the region of micro slip extends to the whole angle of wrap, $\gamma_2 = \alpha_2$, and the region of adhesion becomes zero, $\beta_2 = 0$, c.f. Fig. 2b A further differential increase of F_{23} leads to complete slipping between web and roller. For this type of slip the expression *"macro slip"* is introduced. The ratio of web forces is constant in this case, because α_2 is constant. In steady-state as well as in dynamic motion the Euler-Eytelwein equation now reads as

$$\frac{F_{23}(t)}{F_{12}(t)} = \exp[\mu_2\alpha_2 sign(\frac{F_{23}(t)}{F_{12}(t)} - 1)] = \frac{1}{k_{\alpha 2}} = const_t = \frac{\overline{F}_{23}}{\overline{F}_{12}} \qquad \{6.1\}$$

The roller velocity $\tilde{v}_{c2}(t)$ is without influence now. Two different cases have to be taken into account:

$$\begin{aligned} k_{\alpha 2} &= \frac{\overline{F}_{12}}{\overline{F}_{23}} > 1 \quad \textit{the roller drives the web} \\ k_{\alpha 2} &= \frac{\overline{F}_{12}}{\overline{F}_{23}} < 1 \quad \textit{the web drives the roller}. \end{aligned} \tag{6.2}$$

As has been shown in [11] the following equations are now valid:

$$\frac{\tilde{F}_{23}(s)}{\overline{A}_e \overline{E}} = \frac{1}{1+T_{G13}s} \left[\begin{array}{l} \dfrac{\tilde{F}_{01}(s)}{\overline{A}_e \overline{E}} + (\overline{\varepsilon}_{12} - \overline{\varepsilon}_{01})\tilde{z}_{TE1}(s) \\ +(\overline{\varepsilon}_{23} - \overline{\varepsilon}_{12})\tilde{z}_{TE2}(s) + \dfrac{\tilde{v}_{c3}(s) - \tilde{v}_{c1}(s)}{\overline{v}} \end{array} \right] \tag{6.3}$$

$$\tilde{F}_{12}(s) = k_{\alpha 2}\tilde{F}_{23}(s) \tag{6.4}$$

with

$$T_{G13} = k_{\alpha 2}T_{12} + T_{23} \tag{6.5}$$

In contrast to micro slip, only one common time constant T_{G13} is valid for both web spans in the case of macro slip. The equations for the register errors can be calculated as

$$\tilde{Y}^*_{12}(s) = \frac{\overline{v}}{s}\left[-(1+T_{23}s)\tilde{\varepsilon}_{F23} + e^{-T_{12}s}\tilde{\varepsilon}_{F01} + (\overline{\varepsilon}_{F23} - \overline{\varepsilon}_{F01})e^{-T_{12}s}\tilde{z}_{TE1} + \frac{\tilde{v}_{c3}(s)}{\overline{v}} \right] \tag{6.6}$$

$$\tilde{Y}^*_{13}(s) = \frac{\overline{v}}{s}\left[-\tilde{\varepsilon}_{F23} + e^{-T_{13}}\tilde{\varepsilon}_{F01} + (\overline{\varepsilon}_{F23} - \overline{\varepsilon}_{F01})e^{-T_{13}s}\tilde{z}_{TE1} + \frac{\tilde{v}_{c3}(s)}{\overline{v}} \right] \tag{6.7}$$

With these equations the block diagram of Fig. 2c can be constructed. At the transition point from micro to macro slip the system changes its structure. Göb and Hahn [19] have extended the Euler-Eytelwein equation and achieve a smooth transition. Measured results with roller 5, 6, and 7 of Fig. 1, which were carried out with a modern commercial printing press, are shown on Fig. 10 and 11. Evaluating these figures one is surprised that the simulated and the experimental curves coincide very well. Measured step responses like these indicate significantly that macro slip of the web occurs on a driven roller. If, however, an air cushion is entrained between roller and web these curves will change their shape completely (see, e.g., [20]).

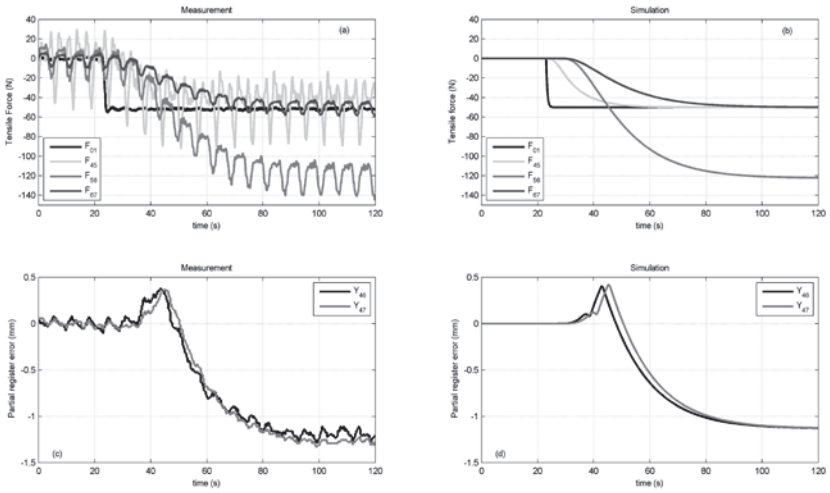

Figure 10 – Step responses with macro-slip, $k_{\alpha 2} > 1$. Left: Measurement. Right: Simulation. Web forces (a), (b) and partial register errors (b), (c), (asterisk not printed)

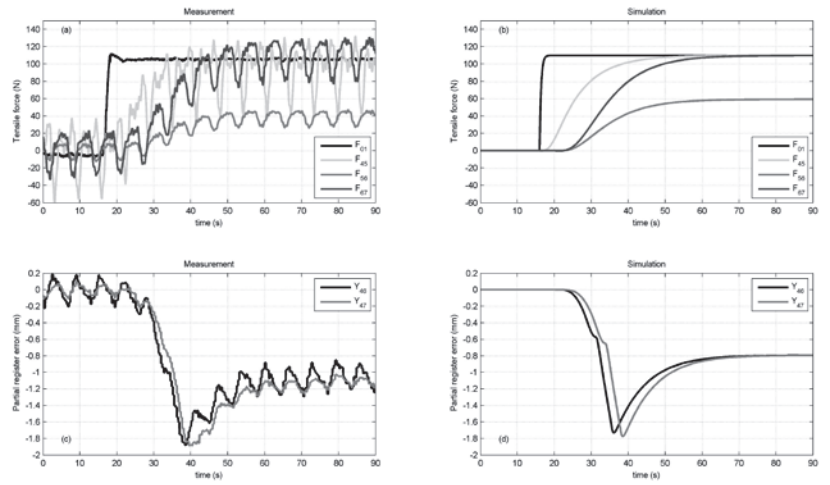

Figure 11 – Step responses with macro-slip, $k_{\alpha 2} < 1$. Left: Measurement. Right: Simulation. Web forces (a), (b) and partial register errors (b), (c), (asterisk not printed)

7. ROLLERS WITH PARTIAL SLIP - THE q-MODEL

System

In the case of touch-sensitive surfaces as, e.g., a printed paper web, covered contact rolls are used, which press the web against the steel roller only on non-image areas (see Fig. 12). Only in these narrow contact zones forces are transferred to the web, whereas the web only touches the steel roller slightly between these zones and is, therefore,

virtually free of any forces there. In order to develop a mathematical model for this complex problem, which can be easily handled, it is assumed that the steel roller impresses its circumferential velocity to the web within the narrow contact areas, whereas the web slips relatively to the steel roller in the area between these pressure rolls. These roller combinations are termed “rollers with partial slip”.

Experiments have shown, that these rollers could not be described with the theory developed until now. It has been observed that changes of F_{01} (c. f. Fig. 1 and Fig. 4), as have been discussed in sections 1 and 4, are not transferred to web span 1-2 with full magnitude. Changes of v_{c2} do not influence the web tension in the upstream span in the same way as pressure rollers of full width do, and a change of tension in the downstream span 2-3 apparently influences the tension in the upstream span 1-2.

It is assumed that the velocity profile $v_x(x = l_{12}, y)$ of the web is approximately shaped as shown in Fig. 12 (with $v_{c3} > v_{c1}$). The strain is shaped similarly. At the input line of roller 2 the velocity profile is non-homogeneous. At positions $x \neq l_{12}$, e.g. at line AA' or BB', it becomes increasingly more homogeneous (principle of Saint Venant). Thus it is assumed, that the length of this inhomogeneous zone is small compared to the web lengths l_{12} and l_{23}, and that the web can be substituted through a web with homogeneous distribution of stress and strain. This will be shown in the next paragraph.

The Steady-State q-Model

The inhomogeneous lateral velocity distribution at the input of roller 2 is replaced by its mean value

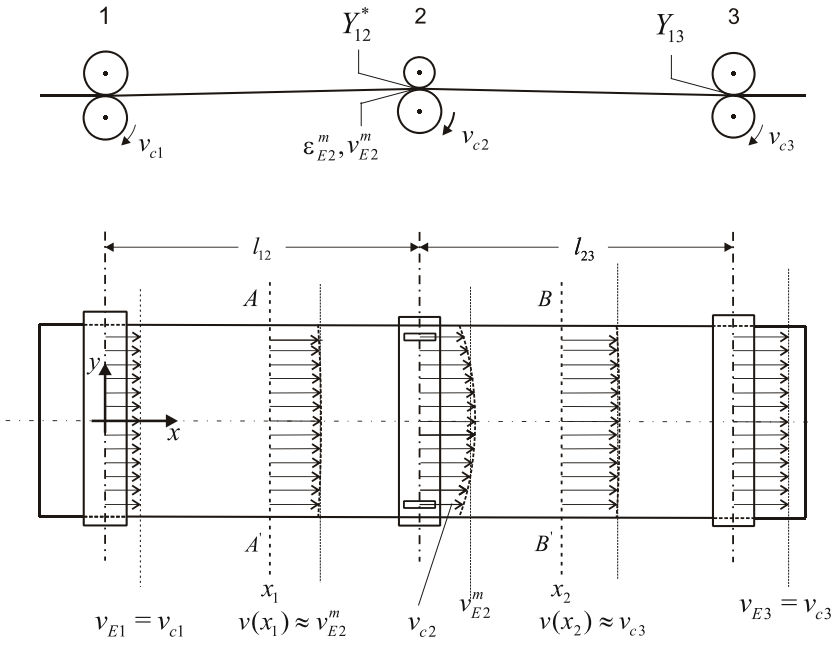

Fig. 12 – Approximated velocity profile of a web transported by a roller 2 with partial slip between rollers 1 and 3 with micro slip

$$v_{E2}^{m} = \frac{1}{b_e} \int_{-b_e/2}^{+b_e/2} v_y(x = l_{12}, y)dy \qquad \{7.1\}$$

which is constant over the web width and uniformly distributed over the cross section, b_e being the width of the tensionless web. The respective mean value of the strain is

$$\varepsilon_{E2}^{m} = \frac{1}{b_e} \int_{-b_e/2}^{+b_e/2} \varepsilon_y(x = l_{12}, y)dy \qquad \{7.2\}$$

Furthermore it is assumed, that roller 2 only transfers the fractional amount $q_2 v_{c2}$, with $0 < q_2 \leq 1$, of its circumferential speed to the web. Then

$$\overline{v}_{E2}^{m} = q_2 \overline{v}_{c2} \qquad \{7.3\}$$

holds.

The recursive steady-state q-model. The three roller system of Fig. 12, consisting of roller 2 with partial slip, the ideal printing unit 1 and the ideal cutting cylinder 3, both of which are assumed with micro slip, is taken for granted.

With $\varepsilon << 1$ the steady-state continuity equation yields the simplified relationships

$$\frac{\overline{v}_{E2}^{m}}{\overline{v}_{c1}} = \frac{1 + \overline{\varepsilon}_{E2}^{m}}{1 + \overline{\varepsilon}_{01}} \approx 1 + \overline{\varepsilon}_{E2}^{m} - \overline{\varepsilon}_{01} \qquad \{7.4\}$$

$$\frac{\overline{v}_{c3}}{\overline{v}_{E2}^{m}} = \frac{1 + \overline{\varepsilon}_{23}}{1 + \overline{\varepsilon}_{E2}^{m}} \approx 1 + \overline{\varepsilon}_{23} - \overline{\varepsilon}_{E2}^{m} \qquad \{7.5\}$$

These equations are necessary and sufficient. Eliminating $\overline{v}_{E2}^{m}$ from {7.4} and {7.5} leads to the relationship

$$\frac{\overline{v}_{c3}}{\overline{v}_{c1}} = \frac{1 + \overline{\varepsilon}_{23}}{1 + \overline{\varepsilon}_{01}} \approx 1 + \overline{\varepsilon}_{23} - \overline{\varepsilon}_{01} \qquad \{7.6\}$$

which is linearly dependent on the first two equations. It shows that the steady-state strain $\overline{\varepsilon}_{23}$ is independent of $\overline{v}_2$. Small stationary deviations (index Δ) are introduced now which lead to the new steady-state

$$\overline{\varepsilon}_{E2\Delta}^{m} \approx \overline{\varepsilon}_{01\Delta} - \frac{\overline{v}_{c1\Delta}}{\overline{v}} + \frac{\overline{v}_{E2\Delta}^{m}}{\overline{v}} \qquad \{7.7\}$$

$$\overline{\varepsilon}_{23\Delta} \approx \overline{\varepsilon}_{E2\Delta}^{m} - \frac{\overline{v}_{E2\Delta}^{m}}{\overline{v}} + \frac{\overline{v}_{c3\Delta}}{\overline{v}} \qquad \{7.8\}$$

$$\boxed{\overline{\varepsilon}_{23\Delta} \approx \overline{\varepsilon}_{01\Delta} - \frac{\overline{v}_{c1\Delta}}{\overline{v}} + \frac{\overline{v}_{c3\Delta}}{\overline{v}}} \qquad \{7.9\}$$

Equations {7.7} and {7.8} clearly show that the web spans 1-2 und 2-3 are connected with each other through $\overline{v}^{m}_{E2\Delta}$ and $\overline{\varepsilon}^{m}_{E2\Delta}$. The mathematical approach linking both quantities is chosen to be

$$\boxed{\frac{\overline{v}^{m}_{E2\Delta}}{\overline{v}} = q_{12}\overline{\varepsilon}^{m}_{E2\Delta} + q_2\frac{\overline{v}_{c2\Delta}}{\overline{v}} + q_{23}\overline{\varepsilon}_{23\Delta}} \qquad \{7.10\}$$

In this formula q_{12} takes into account a possible influence of $\overline{\varepsilon}^{m}_{E2\Delta}$ on $\overline{v}^{m}_{E2\Delta}$, q_2 considers the imperfect transfer of the roller speed $\overline{v}_{c2}$ to the web, and q_{23} is provided in order to describe the retroaction of $\overline{\varepsilon}_{23\Delta}$ on span 1-2. At a later stage the amount and sign of the q-factors will be discussed.

Equation {7.10} must satisfy the continuity equation {7.7}:

$$\boxed{\overline{\varepsilon}^{m}_{E2\Delta} = \overline{\varepsilon}_{01\Delta} + \frac{\overline{v}^{m}_{E2\Delta} - \overline{v}_{c1\Delta}}{\overline{v}}} \qquad \{7.11\}$$

The equations {7.9}, {7.10}, and {7.11} define the *recursive steady-state q-model of roller 2 with partial slip* between the ideal rollers 1 and 3 with micro slip. In these equations $\overline{v}^{m}_{E2\Delta}$ is a function of the dependent variables $\overline{\varepsilon}^{m}_{E2\Delta}$ and $\overline{\varepsilon}_{23\Delta}$, and $\overline{\varepsilon}^{m}_{E2\Delta}$ is a function of the dependent variable $\overline{v}^{m}_{E2\Delta}$.

The non-recursive steady-state q-model. Inserting {7.10} into {7.11} gives

$$\overline{\varepsilon}^{m}_{E2\Delta} = \frac{1}{1-q_{12}}\left(\overline{\varepsilon}_{01\Delta} - \frac{\overline{v}_{c1\Delta}}{\overline{v}} + q_2\frac{\overline{v}_{c2\Delta}}{\overline{v}} + q_{23}\overline{\varepsilon}_{23\Delta}\right) \qquad \{7.12\}$$

and inserting {7.9} into this equation leads to

$$\overline{\varepsilon}^{m}_{E2\Delta} = \frac{1+q_{23}}{1-q_{12}}\left(\overline{\varepsilon}_{01\Delta} - \frac{\overline{v}_{c1\Delta}}{\overline{v}}\right) + \frac{q_2}{1-q_{12}}\frac{\overline{v}_{c2\Delta}}{\overline{v}} + \frac{q_{23}}{1-q_{12}}\frac{\overline{v}_{c3\Delta}}{\overline{v}} \qquad \{7.13\}$$

The following coefficients are defined:

$$A = \frac{1+q_{23}}{1-q_{12}} \qquad \{7.14\}$$

$$B = \frac{q_2}{1-q_{12}} \qquad \{7.15\}$$

$$C = \frac{q_{23}}{1-q_{12}} \qquad \{7.16\}$$

Then {7.13} takes the form

$$\boxed{\bar{\varepsilon}^{m}_{E2\Delta} = A\left(\bar{\varepsilon}_{01\Delta} - \frac{\bar{v}_{c1\Delta}}{\bar{v}}\right) + B\frac{\bar{v}_{c2\Delta}}{\bar{v}} + C\frac{\bar{v}_{c3\Delta}}{\bar{v}}} \qquad \{7.17\}$$

In this equation $\bar{\varepsilon}^{m}_{E2\Delta}$ is a function of the independent variables $\bar{\varepsilon}_{01\Delta}$, $\bar{v}_{c1\Delta}$, $\bar{v}_{c2\Delta}$, and $\bar{v}_{c3\Delta}$.

A corresponding expression for $\bar{v}^{m}_{E2\Delta}$ as a function of the independent variables is found by inserting {7.9} into {7.10}, yielding

$$\frac{\bar{v}^{m}_{E2\Delta}}{\bar{v}} = q_{23}\left(\bar{\varepsilon}_{01\Delta} - \frac{\bar{v}_{c1\Delta}}{\bar{v}}\right) + q_{12}\bar{\varepsilon}^{m}_{E2\Delta} + q_2\frac{\bar{v}_{c2\Delta}}{\bar{v}} + q_{23}\frac{\bar{v}_{c3\Delta}}{\bar{v}} \qquad \{7.18\}$$

Combining this equation with {7.13} leads to the result

$$\boxed{\frac{\bar{v}^{m}_{E2\Delta}}{\bar{v}} = \left(A-1\right)\left(\bar{\varepsilon}_{01\Delta} - \frac{\bar{v}_{c1\Delta}}{\bar{v}}\right) + B\frac{\bar{v}_{c2\Delta}}{\bar{v}} + C\frac{\bar{v}_{c3\Delta}}{\bar{v}}} \qquad \{7.19\}$$

The equations {7.9}, {7.17}, and {7.19} define the *steady-state non-recursive q-model of roller 2* between rollers 1 and 3.

The coefficients A, B und C can serve for measuring of the q-factors with the help of the web tensions in span 1-2 and 2-3. Young's modulus must be known in order to determine the strains. A more elegant and more accurate method is to use the PCREs. This cannot be explained in detail due to confidentiality agreement.

In order to measure the q-factors of a roller with partial slip, this roller must be located between two rollers with micro slip, the one roller printing and the other one non-printing. Hence three angle controlled drives are necessary as well as the sensors for the register marks to be printed. A press has to be adapted to these requirements or an experimental setup has to be provided. This can be costly.

The Dynamic q-Model

In order to find the dynamic behavior of the web, {7.10} is generalized to give the form

$$\frac{v^{m}_{E2}(t)}{\bar{v}} = f\left[\varepsilon_{12}(t), \frac{v_{c2}(t)}{\bar{v}}, \varepsilon_{23}(t)\right] \qquad \{7.20\}$$

By differentiating this function with respect to the tree variables, using the continuity equations of the web spans, and introducing the q-factors q_{12}, q_2 and q_{23} (c.f. Appendix) the following *dynamic recursive q-Model of velocities and strains* for the roller 2 with partial slip results:

$$\boxed{\frac{\tilde{v}^{m}_{E2}}{\bar{v}} = q_{12}\left(1+0.5T_{12}s\right)\varepsilon^{m}_{E2} + q_2\frac{\tilde{v}_{c2}}{\bar{v}} + q_{23}\left(1+T_{23}s\right)\tilde{\varepsilon}_{23}} \qquad \{7.21\}$$

$$\boxed{\tilde{\varepsilon}_{E2}^{m} = \frac{1}{1+T_{12}s}\left(\tilde{\varepsilon}_{01} - \frac{\tilde{v}_{c1}}{\overline{v}} + \frac{\tilde{v}_{E2}^{m}}{\overline{v}}\right)} \qquad \{7.22\}$$

$$\boxed{\tilde{\varepsilon}_{23} = \frac{1}{1+T_{23}s}\left(\tilde{\varepsilon}_{E2}^{m} - \frac{\tilde{v}_{E2}^{m}}{\overline{v}} + \frac{\tilde{v}_{c3}}{\overline{v}}\right)} \qquad \{7.23\}$$

Fig. 13 shows the block diagram. The time constant $0.5T_{12}$ in {7.21} turned out to be optimally suited for the standard newspaper press which was investigated. Other types of printing presses may exhibit different properties. Hence, it might be adequate to define a time constant κT_{12}, resulting in the alternative equation

$$\frac{\tilde{v}_{E2}^{m}}{\overline{v}} = q_{12}\left(1+\kappa T_{12}s\right)\varepsilon_{E2}^{m} + q_2\frac{\tilde{v}_{c2}}{\overline{v}} + q_{23}\left(1+T_{23}s\right)\tilde{\varepsilon}_{23} \qquad \{7.24\}$$

with $0 < \kappa \le 1$, where κ has to be found experimentally. In the following equations $\kappa = 0.5$ is maintained.

Measured values of the factors q are, e.g., $q_{12} = -3.83$, $q_2 = 0.94$, $q_{23} = 1{,}32$. They are valid only within a confined steady-state operating domain. The measured time constant varied by $(15 \pm 11)\,\%$ in reference to the calculated value of $0.5T_{12}$.

For the three roller system of Fig. 13 the dynamic equations for $\tilde{\varepsilon}_{E2}^{m}$, $\tilde{\varepsilon}_{23}$ and $\tilde{v}_{E2}^{m}/\overline{v}$ as functions of the independent variables, similar to {7.5}, {7.17}, and {7.19}, can be calculated to be

$$\tilde{\varepsilon}_{E2}^{m} = \frac{1}{\left(1-q_{12}\right)\left(1+T_{12}^{*}s\right)}\left[\left(1+q_{23}\right)\left(\tilde{\varepsilon}_{01} - \frac{\tilde{v}_{c1}}{\overline{v}}\right) + q_2\frac{\tilde{v}_{c2}}{\overline{v}} + q_{23}\frac{\tilde{v}_{c3}}{\overline{v}}\right] \qquad \{7.25\}$$

$$\tilde{\varepsilon}_{23} = \frac{1}{\left(1-q_{12}\right)\left(1+T_{12}^{*}s\right)\left(1+T_{23}s\right)}\left\{\begin{array}{l}\left[1-q_{12}\left(1+0.5T_{12}s\right)\right]\left(\tilde{\varepsilon}_{01} - \frac{\tilde{v}_{c1}}{\overline{v}}\right) - q_2T_{12}s\frac{\tilde{v}_{c2}}{\overline{v}} \\ +\left(1-q_{12}\right)\left(1+\frac{1-0.5q_{12}}{1-q_{12}}T_{12}s\right)\frac{\tilde{v}_{c3}}{\overline{v}}\end{array}\right\} \qquad \{7.26\}$$

$$\frac{\tilde{v}_{E2}^{m}}{\overline{v}} = \frac{1}{\left(1-q_{12}\right)\left(1+T_{12}^{*}s\right)}\left[\begin{array}{l}\left(q_{12}+q_{23}\right)\left(1+\frac{0.5q_{12}}{q_{12}+q_{23}}T_{12}s\right)\left(\tilde{\varepsilon}_{01} - \frac{\tilde{v}_{c1}}{\overline{v}}\right) + \left(1+T_{12}s\right)q_2\frac{\tilde{v}_{c2}}{\overline{v}} \\ +q_{23}\left(1+T_{12}s\right)\frac{\tilde{v}_{c3}}{\overline{v}}\end{array}\right] \qquad \{7.27\}$$

with

$$T_{12}^{*} = \frac{1 - 0.5q_{12} + q_{23}}{1 - q_{12}} T_{12} \qquad \{7.28\}$$

This is the *dynamic non-recursive q-model* of roller 2. These equations yield the same steady values of the step responses as equations {7.14} to {7.16}.

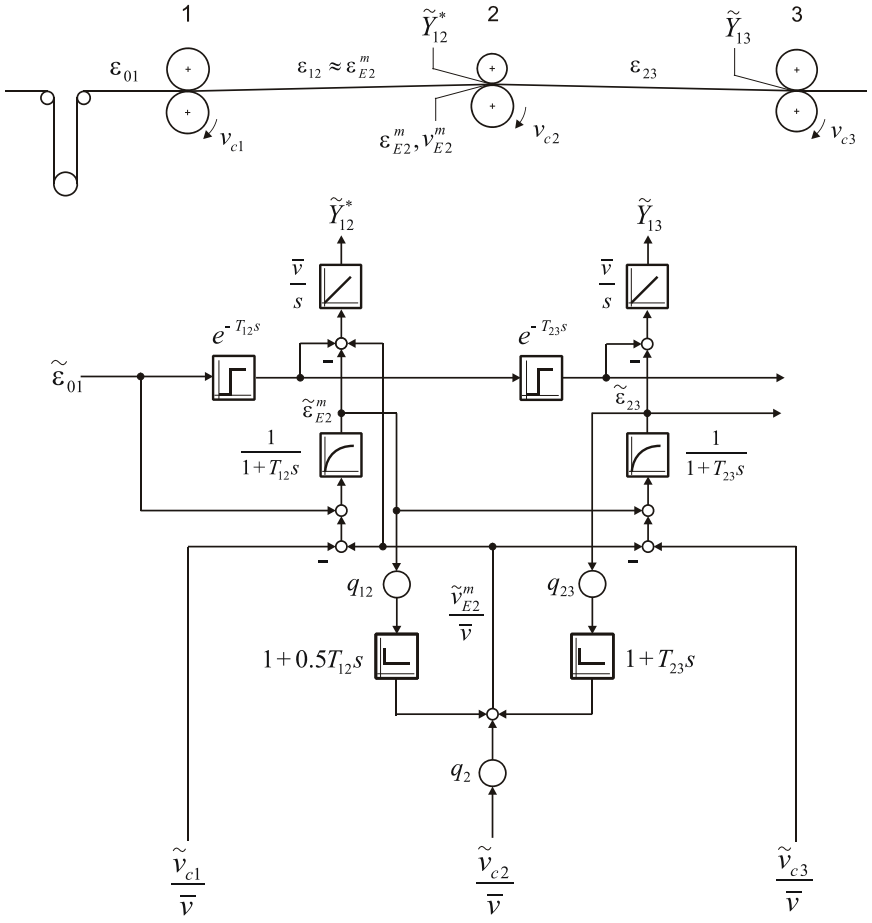

Fig. 13 – Block diagram of roller 2 with partial slip between printing roller 1 and cutting roller 3 with micro slip

Dynamic q-Model of the Cutting Register Errors

It can be proven that $\tilde{\varepsilon}_{E2}$ must be replaced through $\tilde{\varepsilon}_{E2}^{m}$ and $\tilde{v}_{c2}$ through $\tilde{v}_{E2}^{m}$ in the equation of the partial register error {3.1}. With $\tilde{\varepsilon}_{E1} = \tilde{\varepsilon}_{01}$ {3.1} reads as

$$\tilde{Y}_{12}^{*} = \frac{\overline{v}}{s}\left(-\tilde{\varepsilon}_{E2}^{m} + \tilde{\varepsilon}_{01}e^{-T_{12}s} + \frac{\tilde{v}_{E2}^{m}}{\overline{v}}\right) \qquad \{7.29\}$$

The TCRE at the cutting cylinder 3 is the same as before, c.f. {4.1}, if micro slip is assumed for nip 3, as said above,

$$\tilde{Y}_{13} = \frac{\overline{v}}{s}\left(-\tilde{\varepsilon}_{23} + e^{-(T_{12}+T_{23})s}\tilde{\varepsilon}_{01}\right) \qquad \{7.30\}$$

These equations lead to the upper part of the block diagram Fig. 13.

It is interesting to compare the step responses due to changes of ε_{01} and v_{c2} with those of section 4 now.

a) Step function of $\tilde{\varepsilon}_{01}$

Equations {7.25} and {7.27} give

$$\tilde{\varepsilon}_{E2}^{m} = \frac{1+q_{23}}{\left(1-q_{12}\right)\left(1+T_{12}^{*}s\right)}\tilde{\varepsilon}_{01} \qquad \{7.31\}$$

$$\frac{\tilde{v}_{E2}^{m}}{\overline{v}} = \frac{q_{12}+q_{23}}{\left(1-q_{12}\right)\left(1+T_{12}^{*}s\right)}\left(1+\frac{0.5q_{12}}{q_{12}+q_{23}}T_{12}s\right)\tilde{\varepsilon}_{01} \qquad \{7.32\}$$

These relationships have to be inserted into {7.29}. If {4.11} is taken into account

$$\tilde{Y}_{13\infty} = \tilde{Y}_{12\infty}^{*} = \frac{q_{12}+q_{23}}{1-q_{12}}l_{12}\hat{\varepsilon}_{01} \qquad \{7.33\}$$

is obtained after some lengthy calculation. Comparing this equation to {4.9} it can be seen that the PCRE is no longer self compensating. Hence, the new result is: A roller with partial slip causes a sustained PCRE if ε_{01} changes. For $q_{12} = q_{23} = 0$ the PCRE $\tilde{Y}_{12\infty}^{*} = 0$ results.

b) Step function of $\tilde{v}_{c2}$

In this case {7.25} and {7.27} yield

$$\tilde{\varepsilon}_{E2}^{m} = \frac{q_2}{\left(1-q_{12}\right)\left(1+T_{12}^{*}s\right)}\frac{\tilde{v}_{c2}}{\overline{v}} \qquad \{7.34\}$$

and

$$\frac{\tilde{v}_{E2}^{m}}{\overline{v}} = \frac{\left(1+T_{12}s\right)q_2}{\left(1-q_{12}\right)\left(1+T_{12}^{*}s\right)}\frac{\tilde{v}_{c2}}{\overline{v}} \qquad \{7.35\}$$

Inserting these equations into {7.29} the realationship

$$\boxed{\tilde{Y}^*_{12\infty} = \frac{q_2}{1-q_{12}} l_{12} \frac{\hat{v}_{c2}}{\overline{v}}} \qquad \{7.36\}$$

is obtained after lengthy calculations. The slope of $\tilde{Y}^*_{12\infty} = f(\hat{v}_{c2}/\overline{v})$ has changed compared to {4.12}. For $q_2 = 1$ and $q_{12} = 0$, {7.36} transitions into {4.12}.

The equations of the q-model, as far as have been derived until now, can be extended to describe the influence of transport disturbances (c.f. Section 1). In doing so, ε has to be replaced through ε_F. Mostly the steady-state Young's modulus $\overline{E}$ can be assumed to be constant in the various spans where rollers with partial slip are used to transport the web, because the web is dry there. A detailed discussion is not possible within this frame.

In systems with several successive rollers with partial slip the q-model has to be extended. Assuming three rollers with partial slip, roller k positioned between rollers $(k-1)$ and $(k+1)$, it must be taken into account that $\tilde{\varepsilon}^m_{Ek}$ influences both the upstream span and the downstream span. Hence, factors $q^u_{(k-1),k}$ for upstream and $q^d_{k,(k+1)}$ for downstream have to be introduced, giving the following generalized *dynamic recursive q-model* equations:

$$\boxed{\frac{\tilde{v}^m_{Ek}}{\overline{v}} = q^d_{k-1,k}\left(1 + \frac{T_{k-1,k}}{2}s\right)\tilde{\varepsilon}^m_{Ek} + q_k \frac{\tilde{v}_{ck}}{\overline{v}} + q^u_{k,k+1}\left(1 + T_{k,k+1}s\right)\tilde{\varepsilon}^m_{Ek+1}} \qquad \{7.37\}$$

$$\boxed{\tilde{\varepsilon}^m_{Ek} = \frac{1}{1+T_{k-1,k4}s}\left(\tilde{\varepsilon}^m_{Ek-1} + \frac{\tilde{v}^m_{Ek} - \tilde{v}^m_{Ek-1}}{\overline{v}}\right)} \qquad \{7.38\}$$

$$\boxed{\tilde{Y}^*_{1k} = \frac{\overline{v}}{s}\left(-\tilde{\varepsilon}^m_{Ek} + \tilde{\varepsilon}_{01}e^{-T_{1k}s} + \frac{\tilde{v}^m_{Ek}}{\overline{v}}\right)} \qquad \{7.39\}$$

Due to the effort mentioned in chapter 7.2, which is necessary for the measurement of the q-factors, it is recommended to regard several rollers in series as a single unit and to apply the equations to this whole unit. It must be mentioned that pin cylinders in offset printing presses require additional simplifying assumptions.

The Benefit of the q-Model

The q-model provides a better interpretation of the measured web dynamics in the spans which follow the draw roller nip 6 (in Fig. 1) of the turn over device. An improved guidance control of the respective rollers during acceleration and deceleration of a press seems to be possible. From the point of view of technical mechanics the q-model is only a rough approximation, it might be sufficiently precise, however, for control purposes. It is a further step into the direction of achieving the mathematical modelling of the complete printing press.

PART 3 NEW CONTROL STRATEGIES

8. TWO-VARIABLE CONTROL OF WEB FORCES AND CUTTING REGISTER ERRORS

The simplified scheme of Fig. 15a is chosen for the following.

Conditions of the Printing Press

Equation {3.2} shows that the PCRE $\tilde{Y}_{1n}^{*}$ can be influenced through the circumferential velocity $\tilde{v}_{cn}$ of that roller at which the PCRE is measured. In case of the 3-roller-system of Fig. 15a with $n = 3$, {3.2} reads as

$$\tilde{Y}_{13}^{*}(s) = \frac{\overline{v}}{s}\left[-\tilde{\varepsilon}_{E3}(s) + \tilde{\varepsilon}_{E1}(s)e^{-T_{13}s} + \frac{\tilde{v}_{c3}(s)}{\overline{v}} \right] \qquad \{8.1\}$$

It may be assumed that the strain in section 0-1 as well as the strain in section 2-3 are solely functions of time t and not of position x, because the actual printing process is virtually completed, and the paper is dry when it has left nip 2 (c.f. Fig 1, rollers 4, 5, 6, and 8). In section 0-1 the unwound paper is also dry. Hence $\tilde{\varepsilon}_{E1} = \tilde{\varepsilon}_{01}$ and $\tilde{\varepsilon}_{E3} = \tilde{\varepsilon}_{23}$ is valid, and with {3.4} the equation

$$\begin{aligned} \tilde{Y}_{13}^{*} &= \frac{\overline{v}}{s}\left(-\tilde{\varepsilon}_{F23} + e^{-T_{13}s}\tilde{\varepsilon}_{F01} + \left(\overline{\varepsilon}_{F23} - \overline{\varepsilon}_{F01}\right)\tilde{z}_{TE3} + \frac{\tilde{v}_{c3}}{\overline{v}} \right) \\ &= \frac{\overline{v}}{s}\left(-\frac{\tilde{F}_{23}}{\overline{A}_e\overline{E}_{23}} + e^{-T_{13}s}\frac{\tilde{F}_{01}}{\overline{A}_e\overline{E}_{01}} + \left(\overline{\varepsilon}_{F23} - \overline{\varepsilon}_{F01}\right)e^{-T_{13}s}\tilde{z}_{TE1} + \frac{\tilde{v}_{c3}}{\overline{v}} \right) \end{aligned} \qquad \{8.2\}$$

is obtained. Eq. {1.10} yields the expression

$$\begin{aligned} \tilde{\varepsilon}_{F23} &= \frac{1}{1+T_{23}s}\left[\tilde{\varepsilon}_{F12} + \frac{\tilde{v}_{c3} - \tilde{v}_{c2}}{\overline{v}} + (\overline{\varepsilon}_{F23} - \overline{\varepsilon}_{12m})\tilde{z}_{TE2} \right] \\ &= \frac{1}{1+T_{23}s}\left[\tilde{\varepsilon}_{F12} + \frac{\tilde{v}_{c3} - \tilde{v}_{c2}}{\overline{v}} + (\overline{\varepsilon}_{F23} - \overline{\varepsilon}_{12m})e^{-T_{12}s}\tilde{z}_{TE1} \right] \end{aligned} \qquad \{8.3\}$$

Due to the influence of humidity and, above all, of the high temperature in the dryer the steady-state strain $\overline{\varepsilon}_{12}$ is dependent on the position, i.e. $\overline{\varepsilon}_{12} = \overline{\varepsilon}_{12}(x)$. As an approximation, the mean value $\overline{\varepsilon}_{12m} \approx \overline{\varepsilon}_{F12}$ has been introduced in {8.3}. Furthermore, the temperature- and humidity-dependent dynamic part $\tilde{\varepsilon}_{\vartheta 12}(x,t)$ is assumed to be very slow compared to the force dependent strain $\tilde{\varepsilon}_{F12}(t)$ and hence is neglected.

The aim is to control independently the PCRE $\tilde{Y}_{13}^{*}$ and the force $\tilde{F}_{23}$ in the same web span 2-3. Analogous to {1.6} this force is given by $\tilde{F}_{23} \approx \overline{A}_e\overline{E}_{23}\tilde{\varepsilon}_{F23}$. The equations {8.2} and {8.3} clearly show that the variables $\tilde{Y}_{13}^{*}$ and $\tilde{\varepsilon}_{F23}$ are coupled to each other because $\tilde{v}_{c3}$ appears in {8.2} and {8.3}, and $\tilde{\varepsilon}_{F23} = f(\tilde{v}_{c2})$ appears in {8.2}. In order to achieve a stable system, a non-interacting two-variable control has to be designed. Two

manipulated variables are required. It has been shown in [15], that $\tilde{v}_{c3}$ and $\tilde{v}_{c2}$ are appropriate, the latter by reason of the fact, that self-compensation of $\tilde{\varepsilon}_{F23}$ is virtually prevented due to plastic deformation of the hot paper in web span 1-2. Furthermore, measurements have shown that the influence of $\tilde{\varepsilon}_{F12}$ is allowed to be cut off for control design purpose, as is indicated in the block diagram of Fig. 15b. Changes $\tilde{F}_{12}$ are virtually without influence on $\tilde{F}_{23}$. This simplifies the design of the control.

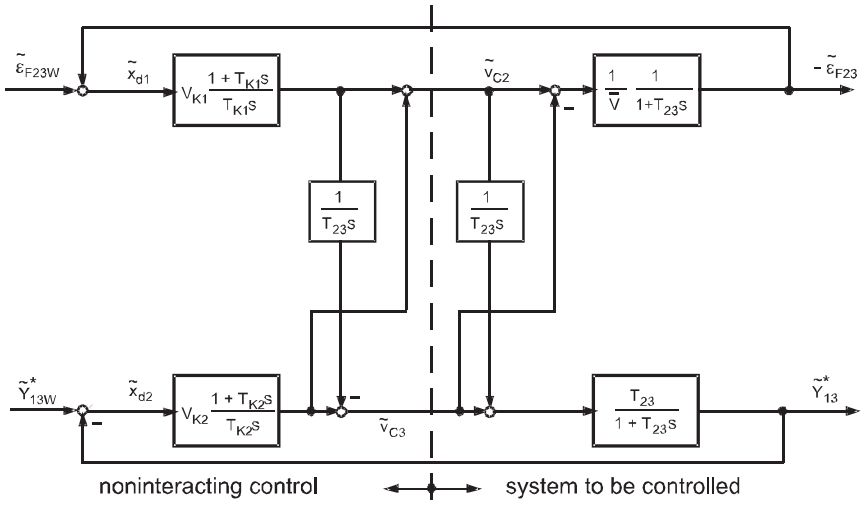

Figure 14 – Result of the design of the two-variable control

Design of the Two-Variable Control

Two controllers together with decoupling networks can be found - by applying Föllinger [21] - in such a way, that two uncoupled closed control loops for $\tilde{\varepsilon}_{F23}$ and $\tilde{Y}^{*}_{13}$ result which can be separately optimized. The calculated decoupling transfer functions (see [13], [14], and [15]), can be simplified in such a way that the cross coupling, which is inherent to the mechanical system to be controlled, is compensated for through the correspondent cross structure - with opposite signs - on the controller side. The resulting structure is illustrated on Fig. 14 with the decoupling elements in the controller and the coupling elements in the system to be controlled.

The decoupling on the mechanical level of the system is shown in Fig. 15c. However, these elements can only be realized on the electronic level of the drives controls (Fig. 15d). The dynamic performance of the actuators, i.e. the speed and angle controlled AC motors with subordinate current controls, has to be taken into account. In doing so, the transfer function of the closed-loop speed control of drive k can be approximately written as

$$G_{e\omega k} = \frac{\tilde{\omega}_k}{\tilde{\omega}_{kw}} \approx \frac{1}{1 + T_{e\omega k} s} \qquad \{8.4\}$$

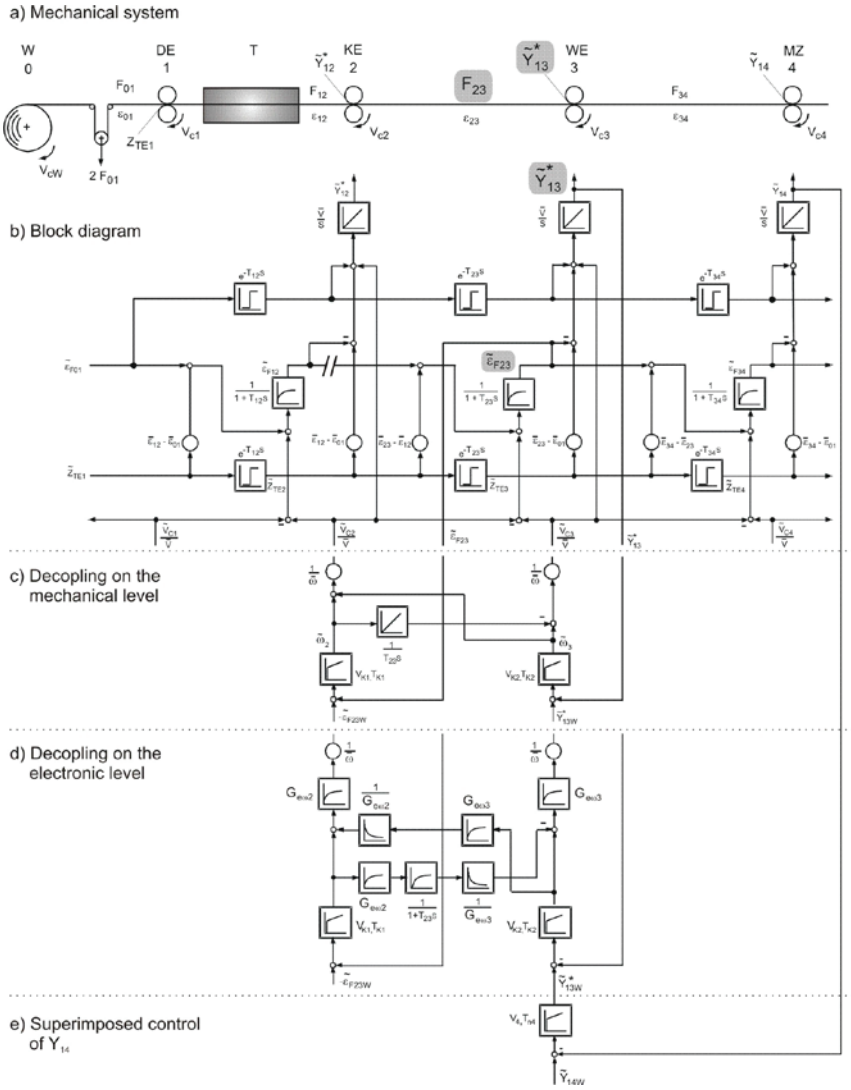

DE four printing units KE chilling unit MZ cutting cylinder
T dryer W unwinder WE draw roller of turner bars

Figure 15 – Rotary offset printing press with decoupled control of web force F_{23} $(\tilde{\varepsilon}_{F23})$ and cutting register errors $\tilde{Y}_{13}^{*}$ and $\tilde{Y}_{14}$

Experiments have shown that the open mechanic integrator $1/(T_{23}s)$ of Fig. 15c, which has to be emulated in the drive electronics, causes instability of the system, because this integrator can never be tuned with sufficient accuracy. Slowly increasing errors would arise which drive the system into instability. Replacing this integrator through a first-order time lag guarantees stability:

$$\frac{1}{T_{23}s} \approx \frac{1}{1+T_{23}s} \qquad \{8.5\}$$

Experimental Results

The new control scheme could be implemented and tested with a commercial offset press of type ROTOMAN produced by manroland, Augsburg (Germany). MATLAB/ SIMULINK proved to be an efficient tool to simulate the press as a system of eight nips as shown in Fig. 1. The chilling unit (nip 5) was modeled as a dead time element, because the areas of adhesion by far exceed the areas of slip on the rollers (c.f. [2] and [6]). According to the measured frequency responses the belt driven roller masses of the chilling unit (nip 2) and of the turner bar unit (nips 6 and 7) together with the appertaining motors can be modeled as elastic two-mass systems. In both cases the closed-loop current controls were approximated through a first-order lag analog to {8.4}, and the speed control loops were optimized without consideration of the influence of the web forces acting as load torques on the motors (c.f. [9]). The speeds of the other nips were assumed to be ideally impressed. The control was implemented on the real time rapid prototyping system SIMULINK/xPC Target. For the data transfer between sensors and actors RS232 interfaces and CAN buses with a cycle time of 3.2 ms were used.

Reference step responses. The measured reference step response of the tensile force $\tilde{F}_{23}$ in Fig.16a shows that the influence of $\tilde{v}_{c2}$ on $\tilde{F}_{12}$ is very small. This performance justifies the assumption of constant tensile force F_{12} mentioned above. The measured deflection of the controlled PCRE $\tilde{Y}_{13}^{*}$ (Fig. 16b) is negligible, which underlines the perfect functioning of the decoupling networks. The reference step response of the $\tilde{Y}_{13}^{*}$ in Fig. 17b is nearly without influence on the controlled tensile force $\tilde{F}_{23}$ (Fig. 17a).

Disturbance responses. When an automatic reel change occurs in the uncontrolled system, the tensile forces $\tilde{F}_{12}$ and $\tilde{F}_{23}$ as well as the PCREs $\tilde{Y}_{12}^{*}$ and $\tilde{Y}_{13}^{*}$ experience high deviations as Fig. 18 shows. The tolerance band of $\pm 0.4\ mm$ is clearly and permanently exceeded. With the new non-interacting control the controlled force $\tilde{F}_{23}$ is driven back to its old reference value (Fig. 19a), and the controlled PCRE $\tilde{Y}_{13}^{*}$ exceeds the tolerance band only during 2.8 s (Fig. 19b). This corresponds to 20 copies of waste paper at the speed of $\overline{v} = 4.31\ ms^{-1} \hat{=} 25000\ ex/h$. This is a considerable improvement compared to the former state of the art of cutting register controls.

Extensions of the Controls

If only $\tilde{Y}_{13}^{*}$ is controlled, it may happen that the steady-state TCRE $\tilde{Y}_{14}$ assumes higher values than in case of the uncontrolled plant. It is essential, therefore, to directly measure the TCRE of the outer paper ribbon of the complete multilayer package as close as possible to the cutting cylinder. Then a closed loop control for $\tilde{Y}_{14}$ is superimposed to the control of $\tilde{Y}_{13}^{*}$ (see Fig. 15e). By this method the best result in reduced waste paper is

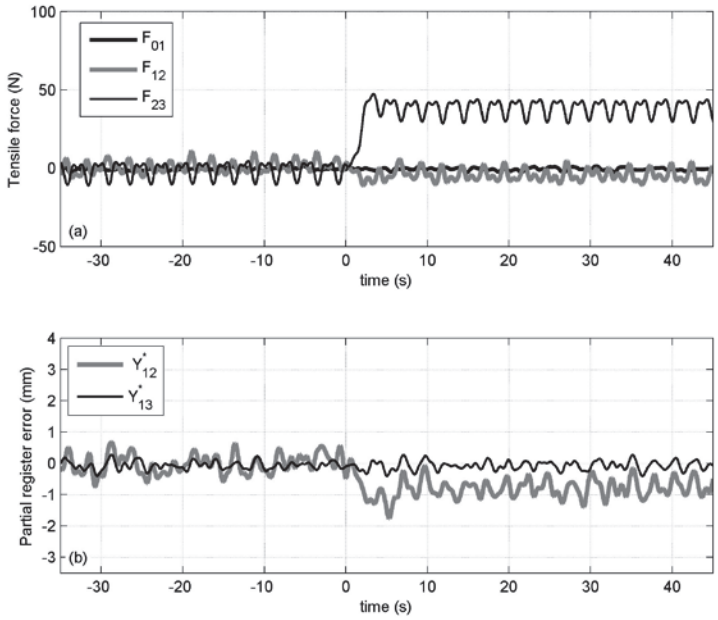

Figure 16 – Reference step response of tensile force F_{23} (a)

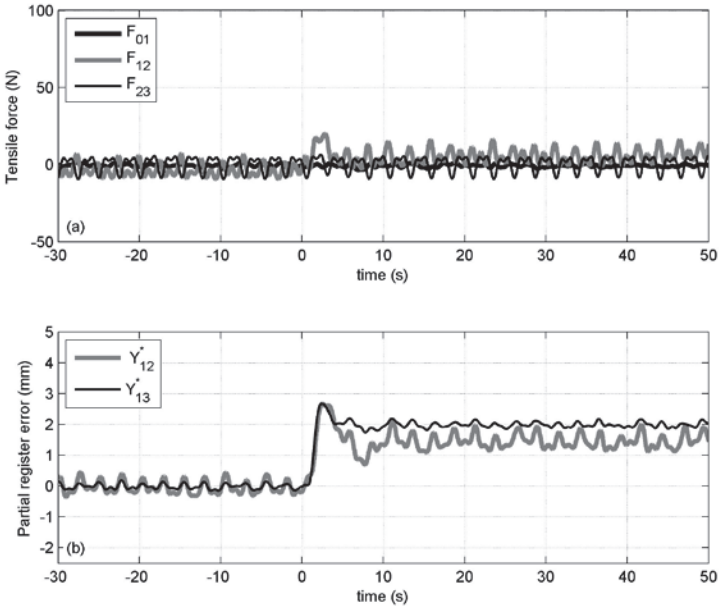

Figure 17 – Reference step response of partial cutting register Y_{13}^{*} (b)

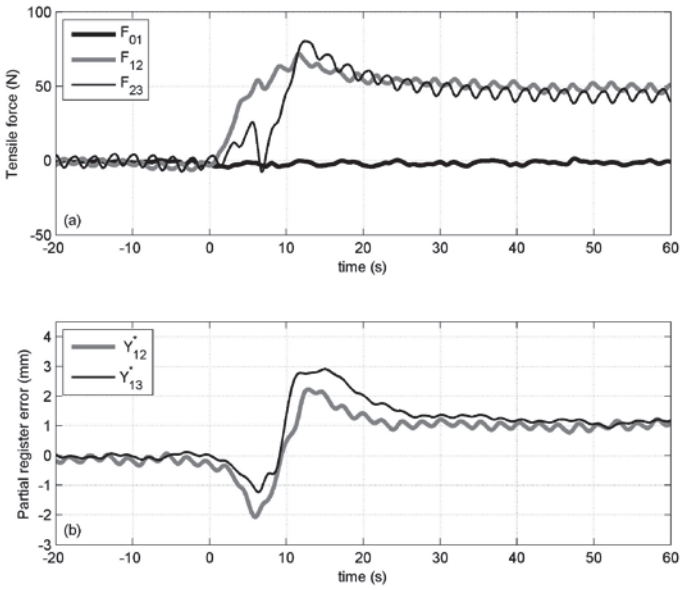

Fig. 18 - Reel change on the run: Tensile forces (a) and partial cutting register errors (b) without control

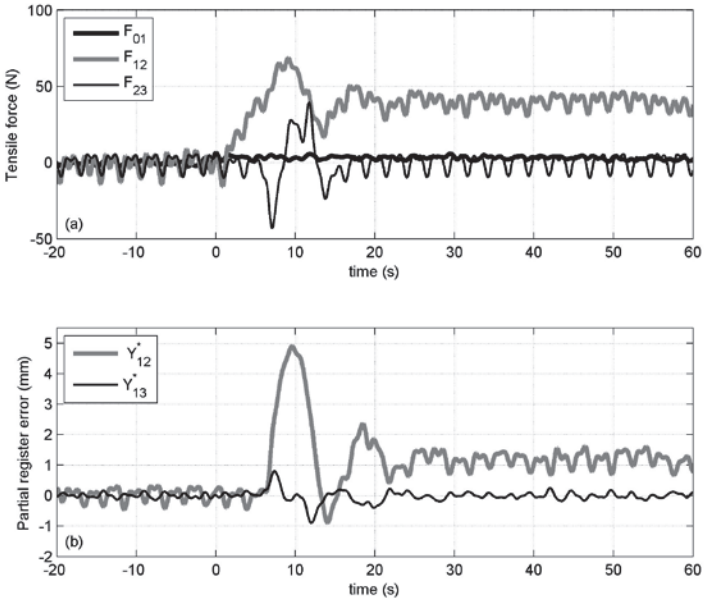

Figure 19 – Reel change on the run: Tensile forces (a) and partial cutting register errors (b) with non-interacting control

achieved. Additionally the PCREs of the other ribbons of the package should be separately controlled.

Furthermore, instead of the chilling unit (nip 2 in Fig. 15a) the four printing units together (nip 1) can serve as manipulated variable. A decoupling is also possible in this case.

The functioning of the non-interacting control has been demonstrated at the rated machine speed of $\overline{v} = 10.3\ m/s \;\square\; 60\,000\ ex/h$.

Another advanced control strategy of the TCRE, described in [22], has been successful on the market.

9. INFLUENCE OF VISCO-ELASTIZITY

As early as in 1973 Tröndle [3] has dealt with a visko-elastic moving web which was expected to be important for the control of web handling systems. Since then no other publication in this area has been published in German. Apparently it has been assumed that the time constants of visco-elastic materials were too big to have any significant influence on modern fast running machines.

Only in 2007 a dissertation [23] appeared by Galle which touched this topic in so far as time constants of plastic foils were measured and classified, but visco-elasticity was not integrated into the process model. The first author to do this with modern numerical methods was Schnabel [24]. He investigated the web tension during the acceleration of a rotogravure press which printed plastic foils. He observed that the tensile force was strongly dependent on the web speed, contrary to the theory. He succeeded in quantitatively explaining the measured behavior and suggested new control strategies. Research in this area is being continued by Göb [25]. These short remarks must be sufficient within the frame of this paper.

EXPRESSION OF THANKS

The author would like to express his appreciation to the responsible persons of Manroland, Augsburg (Germany), who provided him with the unique opportunity of fundamental investigations with industrial rotary printing presses. He is also much obliged to Dr. A. Klemm and Dipl.-Ing. S. Geißenberger, his temporary co-authors, for carrying out measurements and simulations as well as for fruitful discussions and a successful co-operation during many years.

APPENDIX

The Dynamic q-Model

In order to find the dynamics of the web {7.10} is generalized to the form

$$\frac{v_{E2}^{m}(t)}{\overline{v}} = f\left[\varepsilon_{12}(t), \frac{v_{c2}(t)}{\overline{v}_{c2}}, \varepsilon_{23}(t)\right] \qquad \{A1\}$$

At a steady-state operating point $\overline{P}$ the differential can be calculated as

$$df = d\frac{v_{E2}^m}{\overline{v}} = \left[\frac{\partial v_{E2}^m/\overline{v}}{\partial \varepsilon_{12}}\right]_{\overline{P}} d\varepsilon_{12} + \left[\frac{\partial v_{E2}^m/\overline{v}}{\partial v_{c2}/\overline{v}}\right]_{\overline{P}} d\left(\frac{v_{c2}}{\overline{v}}\right) + \left[\frac{\partial v_{E2}^m/\overline{v}}{\partial \varepsilon_{23}}\right]_{\overline{P}} d\varepsilon_{23}$$
$$= f_{12}d\varepsilon_{12} + f_2 d\left(\frac{v_{c2}}{\overline{v}}\right) + f_{23}d\varepsilon_{23} \qquad \{A2\}$$

with the definitions

$$f_{12} = \left[\frac{\partial v_{E2}^m/\overline{v}}{\partial \varepsilon_{12}}\right]_P,\ f_2 = \left[\frac{\partial v_{E2}^m/\overline{v}}{\partial v_{c2}/\overline{v}}\right]_P,\ f_{23} = \left[\frac{\partial v_{E2}^m/\overline{v}}{\partial \varepsilon_{23}}\right]_P \qquad \{A3\}$$

The expression {A2} is not a total differential in the sense of mathematics. This would require a function $v_{E2}^m(t) = v_{E2}^m[\varepsilon_{01}(t), v_{c1}(t), v_{c2}(t), v_{c3}(t)]$, i.e. independent variables in the brackets. But this is the equation we are looking for. Nevertheless, the partial differentiations can be carried out at $\overline{P}$ with respect to one variable by setting constant the other variables – according to the well-known rules.

The partial derivatives are found with the help of the dynamic web equations which can be derived from {1.10} setting $n = 2$, $\tilde{z}_{TEn-1} \equiv 0$ and introducing $\tilde{\varepsilon}_{E2}^m$ instead of $\tilde{\varepsilon}_{E2}^m$ and $\tilde{v}_{E2}^m$ instead of $\tilde{v}_{E2}^m$. Then the two equations

$$\tilde{\varepsilon}_{E2}^m = \frac{1}{1+T_{12}s}\left(\tilde{\varepsilon}_{01} - \frac{\tilde{v}_{c1}}{\overline{v}} + \frac{\tilde{v}_{E2}^m}{\overline{v}}\right) \qquad \{A4\}$$

$$\tilde{\varepsilon}_{23} = \frac{1}{1+T_{23}s}\left(\tilde{\varepsilon}_{E2}^m - \frac{\tilde{v}_{E2}^m}{\overline{v}} + \frac{\tilde{v}_{c3}}{\overline{v}}\right) \qquad \{A5\}$$

are obtained. Rearranging gives

$$\frac{\tilde{v}_{E2}^m}{\overline{v}} = \tilde{\varepsilon}_{E2}^m + \frac{\tilde{v}_{c3}}{\overline{v}} - \left(1+T_{23}s\right)\tilde{\varepsilon}_{23} \qquad \{A6\}$$

$$\frac{\tilde{v}_{E2}^m}{\overline{v}} = \frac{\tilde{v}_{c1}}{\overline{v}} - \tilde{\varepsilon}_{01} + \left(1+T_{12}s\right)\tilde{\varepsilon}_{E2}^m \qquad \{A7\}$$

Both equations are added now in order to achieve one equation in which $\tilde{v}_{E2}^m$ depends on *all* variables. We obtain

$$\frac{\tilde{v}_{E2}^m}{\overline{v}} = \frac{1}{2}\left[\frac{\tilde{v}_{c1}}{\overline{v}} - \tilde{\varepsilon}_{01} + 2\left(1+\frac{T_{12}}{2}s\right)\tilde{\varepsilon}_{E2}^m + \frac{\tilde{v}_{c3}}{\overline{v}} - \left(1+T_{23}s\right)\tilde{\varepsilon}_{23}\right] \qquad \{A8\}$$

Assuming that the variables with tilde are of differential magnitude, the differentials in {A3} can be replaced as follows:

$$d\left(\frac{v_{E2}^m}{\overline{v}}\right)=\frac{\tilde{v}_{E2}^m}{\overline{v}},\ d\varepsilon_{E2}^m=\tilde{\varepsilon}_{E2}^m,\ d\left(\frac{v_{c2}}{\overline{v}}\right)=\frac{\tilde{v}_{c2}}{\overline{v}},\ d\varepsilon_{23}=\tilde{\varepsilon}_{23} \qquad \{A9\}$$

With $\tilde{\varepsilon}_{23}=\tilde{\varepsilon}_{01}=0$ and $\tilde{v}_{c1}=\tilde{v}_{c3}=0$ the function f_{12} defined in {A3} is formulated as

$$f_{12}=\left[\frac{\partial v_{E2}^m/\overline{v}}{\partial\varepsilon_{E2}^m}\right]_{\overline{P}}=\left[\frac{\tilde{v}_{E2}^m/\overline{v}}{\tilde{\varepsilon}_{E2}^m}\right]_{\overline{P}}=1+\frac{T_{12}}{2}s \qquad \{A10\}$$

and for $\tilde{\varepsilon}_{12}=\tilde{\varepsilon}_{01}=\tilde{v}_{c1}=\tilde{v}_{c3}=0$ the function f_{23}

$$f_{23}=\left[\frac{\partial v_{E2}^m/\overline{v}}{\partial\varepsilon_{23}}\right]_{\overline{P}}=\left[\frac{\tilde{v}_{E2}^m/\overline{v}}{\tilde{\varepsilon}_{23}}\right]_{\overline{P}}=-\frac{1}{2}\left(1+T_{23}s\right) \qquad \{A11\}$$

is obtained. The derivative of v_{E2}^m with respect to v_{c2} is heuristically introduced to be

$$\left[\frac{\partial v_{E2}^m/\overline{v}}{\partial v_{c2}/\overline{v}}\right]_{\overline{P}}=\left[\frac{\tilde{v}_{E2}^m/\overline{v}}{\tilde{v}_{c2}/\overline{v}}\right]_{\overline{P}}=q_2 \qquad \{A12\}$$

Factor q_2 equals that in {7.10}. It is assumed that $\tilde{v}_{c2}$ is transferred to v_{E2}^m without any delay.

Then {A8} takes the form

$$\frac{\tilde{v}_{E2}^m}{\overline{v}}=\left(1+\frac{T_{12}}{2}s\right)\varepsilon_{E2}^m+q_2\frac{\tilde{v}_{c2}}{\overline{v}}-\frac{1}{2}\left(1+T_{23}s\right)\tilde{\varepsilon}_{23} \qquad \{A13\}$$

In order to approximate quantitatively the two-dimensional, dynamic lateral and longitudinal velocity and strain profile by the one-dimensional variables $\tilde{v}_{E2}^m$ and $\tilde{\varepsilon}_{E2}^m$ additional degrees of freedom have to be provided. The factors q_{12} und q_{23} are introduced, therefore, which were defined in the steady-state already, c.f. {7.10}. Including the negative sign of $\tilde{\varepsilon}_{23}$ into q_{23} the final equations *dynamic recursive q-model of velocities and strains* can be formulated as shown in chapter 7, equations {7.21} to {7.23}.

REFERENCES

1. Brandenburg, G., Geißenberger, S. et al., "Multi-Motor Electronic Line Shafts for Rotary Offset Printing Presses - a Revolution in Printing Machine Techniques," IEEE/ASME Transactions on Mechatronics, Vol. 4, No. 1, 1999, pp. 25-31.
2. Brandenburg, G., "Über das Verhalten durchlaufender elastischer Stoffbahnenbei Kraftübertragung durch Coulomb'sche Reibung in einem System angetriebener, umschlungener Walzen, " Dr.-Ing.-Dissertation, TH München, 1971.
3. Tröndle, H.P., "Zum dynamischen Verhalten transportierter elastischer und visko-elastischer Stoffbahnen zwischen aufeinanderfolgenden Klemmstellen, " Dr.-Ing. Dissertation, TU München, 1973.

4. Brandenburg, G. and Tröndle, H.-P., “Das Verhalten durchlaufen der elastischer Stoffbahnen bei ortsabhängiger Verteilung von Elastizitätsmodul, Querschnitt und Dichte, ” Siemens Forschungs- und Entwicklungsberichte, Jg. 4, No. 6, 1975, pp. 359-367.
5. Brandenburg, G. and Tröndle, H.-P., “Dynamik des Längsregisters bei Rollenrotationsdruckmaschinen, ” Siemens Forschungs- und Entwicklungsberichte, 5 Nr. 1, pp. 17-20 und Nr. 2, 1976, S. 65-71
6. Brandenburg, G., “New Mathematical Models for Web Tension and Register Error,” Proc. 3. Int. IFAC Conf. on Instrumentation and Automation in the Paper, Rubber and Plastics Industries, PRP 3, Brussels, 1976, pp. 411-438.
7. Brandenburg, G., “Verallgemeinertes Prozessmodell für Fertigungsanlagen mit durchlaufenden Bahnen und Anwendung auf Antrieb und Registerregelung bei Rotationsdruckmaschinen,” Habilitationsschrift, Technische Universität München, 1976. Appeared as shortened version in: Fortschrittberichte der VDI Zeitschriften, Reihe 1, Nr. 46, Düsseldorf, VDI-Verlag 1976.
8. Brandenburg, G. and Karbacher, N., “Ein Beitrag zur Optimierung von Regelkreisen mit Tänzerwalzen bei kontinuierlichen Fertigungsanlagen,” Regelungstechnik (29) 1981, H. 12, S. 428-433; (30) 1982, H. 1, S. 13-21; H. 2, S. 60-64.
9. Kessler, G., Brandenburg, G., Schlosser, W., and Wolfermann, W., “Struktur und Regelung bei Systemen mit durchlaufenden elastischen Bahnen und Mehrmotoren-Antrieben,” Regelungstechnik (32*)* H. 8, 1984, pp. 251-266.
10. Brandenburg, G., Klemm, A. and Seebauer, J., “Online-Rekonstruktion von Elastizitätsmodul-Änderungen der Papierbahn in Rollendruckmaschinen, ” Tagungsband SPS/IPC/ DRIVES, Nürnberg, 2008, VDE-Verlag, Berlin, Offenbach, pp. 461-473.
11. Brandenburg, G., Geißenberger, S., and Klemm, A., “Einfluss von Klemmstellen mit Gleitschlupf auf Zugkräfte und Registerfehler von durchlaufenden Bahnen in kontinuierlichen Fertigungsanlagen, ” Tagungsband VVD 2003, Fachtagung Ver-Verarbeitungs maschinen und Verpackungstechnik, Technische Universität Dresden, pp. 391-411.
12. Brandenburg, G., “Dynamisches Verhalten von Dublier- und Registerfehlern bei Rollenoffset-Druckmaschinen, ” Tagungsband SPS/IPC/DRIVES, Nürnberg 000, Hüthig-Verlag, Heidelberg, pp. 698-715.
13. Brandenburg, G., Geißenberger, S., and Klemm, A., “Entkoppelte Regelung von Bahnzugkraft und Schnittregisterfehlern bei Rollendruckmaschinen mit elektronischer Welle, ” VDI/VDE Tagung Elektrisch-mechanische Antriebssysteme, Fulda, 2004, pp. 273-285.
14. Brandenburg, G., Geißenberger, S., and Klemm, A., “Schnelle Schnittregister- und Bahnzugkraftregelung für Rollendruckmaschinen,” Tagungsband SPS/IPC/ DRIVES, Nürnberg, 2004, pp. 435-447 .
15. Brandenburg, G., S. Geißenberger, S., and Klemm, A., “Non-interacting Control of Web Forces and Cut-off Register Errors in Rotary Printing Presses with Electronic Line Shafts,” EPE Journal*,* Vol. 16, No. 2, 2006, pp. 38-55.
16. Brandenburg, G., “New Mathematical Models and Control Strategies for Rotary Printing Presses and Related Web Handling Systems,” to appear in Trans. IFAC World Congress, Milano, 2011.
17. Manroland AG 2 CUTCON C > CUTCON plus 02 deutsch 03/2009, www.manroland.com, printservices@manroland.com

18. Valenzuela, M. A. , Bentley, J. M. and Lorenz, R. D., “Dynamic online sensing of sheet modulus of elasticity,” IEEE Trans. on Ind. Appl., Vol. 46, No. 1, 2010, pp.108-120.
19. Göb, M. and Hahn, I., “Simulation des Bahnspannungsverhaltens in bahnverarbeitenden Maschinen unter Berücksichtigung von Klemmstellen mit Dehn- und Gleitschlupf,” Tagungsband SPS/IPC/ DRIVES, Nürnberg, 2009, pp. 359-367, VDE-Verlag, Berlin, Offenbach.
20. Ducotey, K. S. and Good, J. K., “The Effect of Web Permeability and Side Leakage on the Air Film Height between a Roller and Web,” Journal of Tribology, Vol. 20, 1998, pp. 559-565.
21. Föllinger, O., Regelungstechnik, 1985, Hüthig-Verlag Heidelberg.
22. Güth, R., Mengiesen, J. C., and Munz, C., “Bildbasierte Schnittlageregelung in der WIFAG evolution 471 und 371,” Evolution, WIFAG Informationsbulletin, No. 36, 2003, Bern (CH), pp. 4-13.
23. Galle, A., “Regelungstechnische Untersuchung der Bedruckstoffförderung in Rollendruckmaschinen,” Dr.-Ing. Dissertation TU Chemnitz, 2007, http://archiv.tu-chemnitz.de/pub/007/0159.
24. Schnabel, H., “Entwicklung von Methoden zur Registerregelung in Abhängigkeit der Bahnzugkraft bei Rollen-Tiefdruckmaschinen,” Dr.-Ing. Dissertation TU Darmstadt, 2009, Sierke-Verlag, Göttingen.
25. Göb, M. and Hahn, I., “Identifikation des Materialverhaltens in kontinuierlichen Fertigungsanlagen,” Tagungsband SPS/IPC/ DRIVES,Nürnberg, 2010, VDE-Verlag, Berlin, Offenbach, pp. 75-83.

Keynote Presentation – *Advanced Process Models and Control Strategies for Rotary Printing Presses*	**Dr. Günther Brandenburg,** Technische Universität, GERMANY

Name & Affiliation	**Question**
Gunther Oedl, Brueckner Machinery	Why is there a periodic deviation in the forces which can be seen in the different simulations?
Name & Affiliation	**Answer**
Günther Brandenburg, Technische Universität München	I cannot tell you precisely because there were several potential sources and there was no time to determine which source or sources were responsible. The dancer roller, some out-of-round or eccentric rollers and the switching of the dryer were among the potential sources. The combination of the influence of the various sources could not be analyzed correctly.
Name & Affiliation	**Question**
Clarence Klassen, KlassEngineering	Often I see a disturbance in a downstream section affecting the tension upstream. Would decoupling control help even if we don't need control of the registration?
Name & Affiliation	**Answer**
Günther Brandenburg, Technische Universität München	We did not apply our control to this problem. The control is provided in the first stage for commercial printing presses. In commercial printing presses, we don't have rollers that are downstream influencing the upstream tension. There are many effects in newspaper printing presses which are very important which we have investigated. The control problem was not part of this research. We have a model now, so now we can study new control theories. It is not urgently needed. There is no money in the industry at the present time due to the present financial crisis and to competition between the internet and newspaper presses.
Name & Affiliation	**Question**
Dilwyn Jones, Emral Ltd.	I am not a controls expert, but I recall from discussion of previous models that inertia was included and was important.
Name & Affiliation	**Answer**
Günther Brandenburg, Technische Universität München	We neglected the influence of inertia. If there are many rollers, you do have an influence. We can investigate the influence of inertia, but it is not part of the decoupled control. I think the influence is relatively small. Otherwise we would not have gotten these fine curves. The influence is negligible.
Name & Affiliation	**Question**
Ron Swanson, 3M Company	One of your visions was more work needs to be done on the dryer. What do you think is happening in the dryer?

Name & Affiliation	Answer
Günther Brandenburg, Technische Universität München	The modulus of elasticity of the web is position and time dependent. The force is only time dependent. There is a profile of temperature in the dryer. The maximum temperature of the web is 180°C and then it is cooled. I am not sure what happens but I think we must model it nonlinearly. The changes are very big because of the dryer's bang-bang control. These disturbances cannot be described by linear models. The models we have developed are linear models which allow us to apply linear control theory. I have asked people what exactly happens in dryers, but they didn't know.